

SEMMELWEIS EGYETEM
DOKTORI ISKOLA

Ph.D. értekezések

3006.

TAKÁCS ANGÉLA

**A gyógyszerészeti tudományok korszerű kutatási irányai
című program**

Programvezető: Dr. Antal István, egyetemi tanár

Témavezetők: Dr. Lajkó Eszter, tudományos főmunkatárs és

Dr. Kőhidai László, egyetemi tanár

THE EFFICACY OF BORTEZOMIB AGAINST A2058 MELANOMA CELL LINE

PhD thesis

Angéla Takács, PharmD

Pharmaceutical Sciences Doctoral School
Semmelweis University



Supervisor: Eszter Lajkó, PharmD, PhD
László Kőhidai, MD, CSc

Official reviewers: Viola Tamási, PharmD, PhD
Lilla Turiák, PharmD, PhD

Head of the Complex Examination Committee: Éva Szökő,
PharmD, DSc

Members of the Complex Examination Committee:
Sándor Kerpel-Fronius, MD, DSc
Imre Klebovich, PharmD, DSc

Budapest
2024

Table of Contents

List of Abbreviations	5
1. Introduction	7
1.1. Combinatorial drug therapies in oncology	7
1.1.1. Preclinical testing methods of antitumor combinatorial therapies	8
1.2. Melanoma	9
1.3. Proteasome inhibitors	10
1.3.1. Bortezomib	11
1.3.1.1. Mechanism of action	11
1.3.1.2. Main side effects: bortezomib-induced peripheral neuropathy	14
1.4. TIC10	15
1.4.1. Mechanism of action	16
2. Objectives	17
3. Methods	18
3.1. Cell culturing	18
3.2. Materials	18
3.3. Viability assays	19
3.3.1. alamarBlue	19
3.3.2. CellTiter-Glo	20
3.3.3. Real-Time Viability Assay: xCELLigence SP	20
3.4. Quantification of interactions between drugs	20
3.5. Apoptosis Assay	20
3.6. Detection of the proteasome activity	21
3.7. Luminescence-based measurement of intracellular H ₂ O ₂ levels	22
3.8. Microscopic detection of intracellular ROS levels	22
3.9. Proteome profiler human apoptosis array kit	23
3.10. Flow Cytometric Detection of Death Receptors	23
3.11. Statistical analysis	24
4. Results	25
4.1. The impact of alpha-lipoic acid and vitamin B1 on the antitumor effects of bortezomib	25
4.1.1. The anti-proliferative effect of bortezomib is decreased by alpha-lipoic acid	25

4.1.2.	The increase in the proteasome activity following co-treatment with ALA + BOZ 20 ng/mL is concentration-dependent	28
4.1.3.	Oxidative status changes after treatment with bortezomib and alpha-lipoic acid compared to the bortezomib treatment	30
4.1.4.	The loss of the antitumor effect may be mediated by the altered apoptotic proteins	34
4.2.	The effects of the combinatorial treatment of TIC10 and bortezomib	36
4.2.1.	TIC10 has no IC50 value on A2058 melanoma cells	36
4.2.2.	Bortezomib and TIC10 were more effective together than the matching monotreatments in A2058 cells	36
4.2.3.	The protein expression of death receptor 5 is increased after bortezomib treatment	41
5.	Discussion	43
6.	Conclusions	49
7.	Summary	50
8.	References	51
9.	Bibliography of the candidate's publications	66
9.1.	List of publications used for the thesis	66
9.2.	List of publications not used for the thesis	66
10.	Acknowledgments	69

List of Abbreviations

7AAD	7-aminoactinomycin
ALA	alpha-lipoic acid
ANOVA	one-way analysis of variance
Ax V	Annexin V
Bcl2	B-cell lymphoma 2 protein
BIPN	bortezomib-induced peripheral neuropathy
BOZ	bortezomib
DISC	death-inducing signaling complex
DMSO	dimethyl sulfoxide
DRD2	G protein-coupled dopamine receptor D2
DRG	dorsal root ganglia
DR4	death receptor 4
DR5	death receptor 5
ECACC	European Collection of Authenticated Cell Cultures
ER	endoplasmic reticulum
ERK	extracellular signal-regulated kinase
FADD	Fas-associated protein with death domain
FDA	Food and Drug Administration
Fisher's LSD	Fishers's Least Significant Difference
FITC	fluorescein isothiocyanate
FLIP	FLICE-inhibitory protein
FOXO3	Forkhead box O3
H ₂ O ₂	hydrogen peroxide
HNSCC	head and neck squamous cell carcinoma
HO-1	heme oxygenase 1
Hsp60	heat shock protein 60
Hsp70	heat shock protein 70
GSH	glutathione-reduced ethyl ester
IC ₅₀	half-maximal inhibitory concentration
IκB	inhibitory kappa B
MCL	mantle-cell lymphoma

MFI	mean fluorescence intensity
NAC	N-acetyl-l-cysteine
NCI	National Cancer Institute
NF- κ B	nuclear factor kappa B
NOXA	Phorbol-12-myristate-13-acetate-induced protein
PBS	phosphate buffered saline
PS	phosphatidylserine
RFI	ratio of the mean fluorescence intensity
SD	standard deviation
TIC10	TRAIL-inducing compound 10
TRAIL	TNF-Related Apoptosis-inducing ligand
UPR	unfolded protein response
vit B1	vitamin B1
XIAP	X-linked inhibitor of apoptosis protein

1. Introduction

1.1. Combinatorial drug therapies in oncology

In 1965, one of the first combinatorial therapies (a combination of methotrexate with 6-mercaptopurine, prednisone with 6-mercaptopurine, and prednisone with vincristine) was launched against acute lymphoblastic leukemia successfully in pediatric patients (1, 2). Combinatorial treatments are well-used in many disease types ever since, e.g., infectious diseases, metabolic and cardiovascular disorders, and last but not least different cancer types (3-7). Due to the simultaneously targeted molecular pathways, the administration of combination therapies results in higher survival rates, improved therapy outcomes, and better quality of life for the treated patients. So, the aim of using combination drug therapies is to increase efficacy while reducing the dose of the single agents thus drug-associated side effects, as well as off-target effects are decreased, while minimizing the possibility of resistance mechanisms (Figure 1) (5, 8-10).

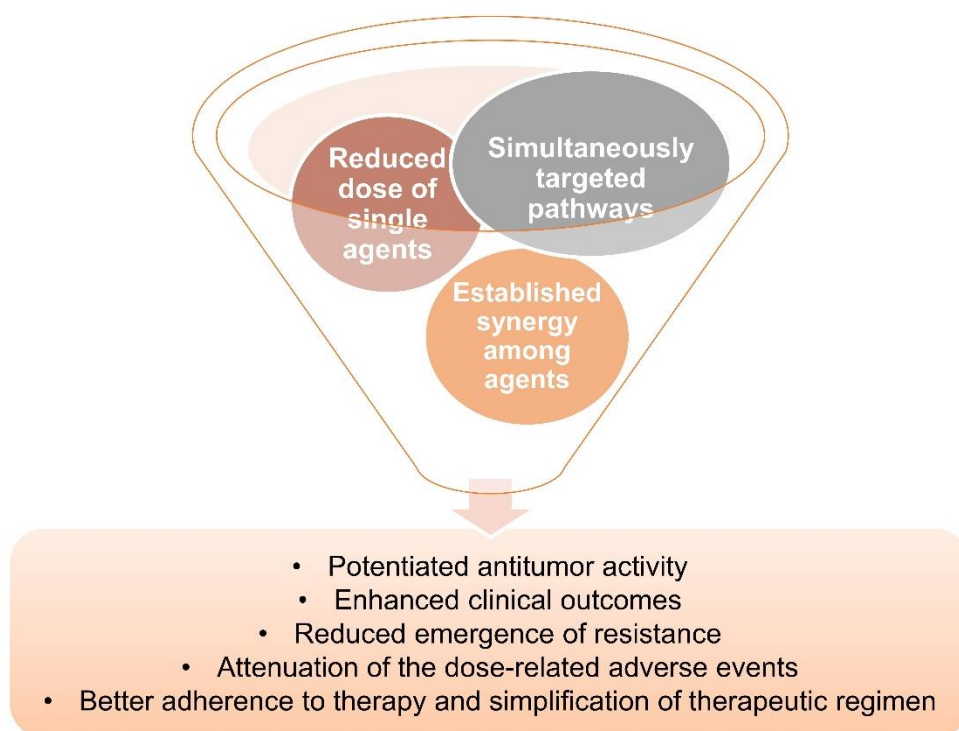


Figure 1 Benefits of antitumor combination therapies

Unfortunately, the use of combinatorial drug therapies can also be challenging as the given medications can differ in their pharmacokinetics, and drug interactions may also occur making the co-administration more difficult (11, 12).

The challenging question is how to select the correct combinations and how to interpret these preclinical results to be able to start a clinical trial where several clinical endpoints are measured, e.g., overall survival as the gold standard value complemented with progression-free survival and time to progression, among others (13).

1.1.1. Preclinical testing methods of antitumor combinatorial therapies

To simplify the selection and to prioritize the correct combinations of drugs and drug candidates, different *in silico* or *in vitro* methods are known. The possible drug combinations are almost endless. There are around 250 already approved cancer drugs on the market. Theoretically, the number of possible two-way combinations is 31,125; regardless of testing the different concentrations (2). One can see, that to be able to handle this huge amount of work and data, next to empirical methods, (i) prediction methods, (ii) computational modeling, (iii) drug libraries, (iv) *in silico* methods and (v) rational designing are essential (14). Since 1928, when the Loewe additivity model was introduced, various models were formed, such as the Bliss independence theorem, the Goldie-Coldman hypothesis, and Chou-Talalay's model (2).

Chou-Talalay's modeling method for predicting drug combinations is based on the mass-action law principle and is the expanded version of the Loewe additivity model (2, 15). This model allows us to recognize different relationships, not only synergism between compounds but additivity and antagonism, too (Figure 2). According to the literature, synergism occurs when the total effect of two or more drugs is greater than the sum of the effects achieved when they are all given individually, antagonism occurs when the total effect of the combinatorial therapy is lower than the effects of the given drugs alone and additivity occurs when the combined effect of drugs given together equals the effects of the drugs given individually (16, 17). Calculating or predicting these interactions between the drugs presents its own challenges. Synergy often occurs from a pharmacological perspective, but mathematically it is hardly provable (17).

In my Ph.D. work, Chou-Talalay's median effect model was used to evaluate the possible interactions (antagonism and synergism, respectively) of the proteasome inhibitor bortezomib (BOZ). Antagonism was studied between alpha-lipoic acid (ALA) + BOZ or vitamin B1 (vit B1) + BOZ. These neuroprotective agents (ALA, vit B1) can help managing the symptoms of side effects related to BOZ (e.g. bortezomib-induced peripheral neuropathy (BIPN)); however, there can be a risk of antagonizing the antitumor

effect of BOZ in melanoma or in myeloma cells. Then, synergism was studied by this model between TRAIL-inducing compound 10 (TIC10) + BOZ against melanoma and myeloma cells, in able to define combinations of these two agents, where the dose of BOZ is minimized while the antitumor efficacy remains with the help of the synergism with TIC10.

We chose Chou-Talalay's median effect model because it is highly cited (over 6000 times according to Researchgate (18), so our results can be compared to the outcomes of experiments performed by other scientific groups and it does not require the knowledge of any programming languages.

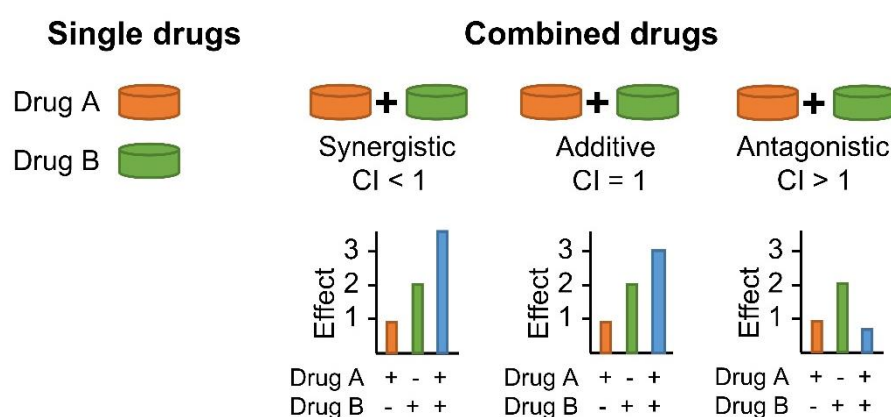


Figure 2 Examples of synergistic, additive, and antagonistic effects evaluated by Chou-Talalay's median effect model (CI: Combination index)

To quantify the relationship, the Combination index (CI) value was created that shows the range of the relationship between the investigated drugs. CI < 1, = 1, and > 1 indicate synergism, additive effect, and antagonism, respectively (19, 20). Chou and his colleagues also developed the free Compusyn software (21), that enables the construction of automated computerized stimulations (22).

1.2. Melanoma

Melanoma is the malignant transformation of the pigment-producing melanocytes that are located in the stratum basale (23). The melanocytes produce melanin (eumelanin and pheomelanin), which is responsible for the basal pigmentation of the skin, eyes, and hair. This phenomenon has a great role in the protection of these organs from DNA-damaging ultraviolet (UV) radiation (24, 25). Unfortunately, epidemiological analyses show that the incidence of melanoma, as well as the mortality, has been rising in Europe.

Both extrinsic, environmental factors and intrinsic, UV-independent mutations are important in the genesis of melanoma (26). The major extrinsic factor is the excessive exposure to solar UV radiation that activates the melanocytes that begin to proliferate uncontrolled and produce an increased amount of UV-absorbing melanin. The genome integrity becomes damaged via reactive oxygen species (ROS), via misincorporation of bases during mitosis, and via depurination or depyrimidination directly initiated by UV radiation (27, 28). Both germline and somatic mutations can play a significant role in the development of melanomas (28, 29). Among patients with hereditary melanoma, the *CDKN2A* mutation has one of the highest frequencies in melanomagenesis (30). The driving somatic mutations that often appear in melanoma malignum are the *BRAF*, the *NFI*, and the *NRAS* genes (31, 32). Melanoma is a highly metastatic disease. The cancerous cells often spread from the primary tumor to different organs, e.g., to subcutaneous tissue, followed by lungs, liver, bones, and brain (33).

The standard treatment of early-stage melanoma is the surgical removal of the tumor and the surrounding normal tissue (29). During the late stage of the disease, when the metastatic cells appear in distant sites of the body, the therapy becomes more difficult, as these cells may have higher genomic variability, although, nowadays there are more treatment options, e.g., chemotherapy, radiotherapy, photodynamic therapy, targeted therapy and last, but not least immunotherapies such as immune checkpoint inhibitors (23, 34). These therapies vary depending on the type of melanoma.

1.3. Proteasome inhibitors

The proteasome can be found in eukaryotic cells (35). It is a protein complex that plays a crucial role in regulating the level of endogenous proteins while establishing protein homeostasis (36). The 19S regulatory subunit and the 20S proteolytic subunit together build the 26S human proteasome. The 20S proteolytic unit is composed of 4 homologous rings, 2 inner β rings, and 2 outer α rings (Figure 3) (37). The regulatory 19S subunit controls the denaturation and the polyubiquitination of the proteins that then must pass through a narrow opening formed by the α rings to be catalytically degraded in the lumen of the 20S complex. There are 3 proteolytic active sites of the β rings inside the lumen - $\beta 1$ (caspase-like), $\beta 2$ (trypsin-like), and $\beta 5$ (chymotrypsin-like) (38, 39).

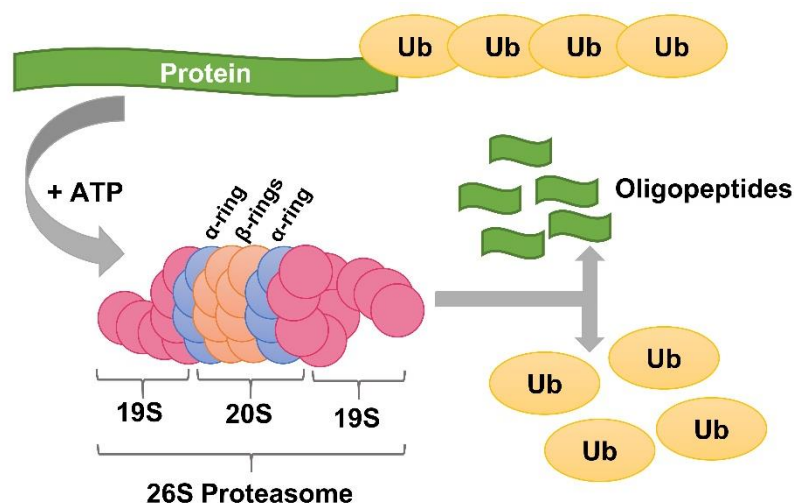


Figure 3 The ubiquitin (Ub)-proteasome system (based on (40))

Before the proteins enter the 26S proteasome, they need to be tagged by a covalently linked polyubiquitin moiety in a multistep enzymatic process (41). By the non-lysosomal degradation of a protein via the ubiquitin-proteasome pathway, a wide range of cellular processes can be tightly regulated. Among these proteins, there are regulators of the cell cycle, cell division, DNA repair, and last but not least tumor suppressor proteins (37, 42, 43). In addition, it has been found that in cancerous transformation enhanced proteasomal activity can contribute to pro-survival activities (43, 44). Therefore, the development and use of proteasome inhibitors are beneficial in antitumor therapy (45).

The proteasome inhibitors can be natural or synthetic (46). The spice curcumin and green tea polyphenols are considered to be natural (47, 48). The first synthetic proteasome inhibitors were peptide-aldehyde derivatives, e.g. MG-132: Z-Leu-Leu-Leu-CHO but the selectivity of these compounds was not high enough, they could interact with other enzymes, e.g., serine and cysteine proteases such as cathepsins and calpains (49, 50). The first targeted proteasome inhibitor already investigated in clinical trials is BOZ (51).

1.3.1. Bortezomib

1.3.1.1. Mechanism of action

Bortezomib is a low molecular weight water-soluble dipeptide boronic acid derivative (52). It can selectively and reversibly bind to the N-terminal threonine in the $\beta 5$ subunit within the 20S proteasome, leading to the inhibition of the chymotrypsin-like proteasomal activity (53).

In the United States, the Food and Drug Administration (FDA) approved BOZ as a single agent for use in multiple myeloma after two unsuccessful treatments in 2003 (54). In 2004, it was also authorized for use in the treatment of relapsed and refractory multiple myeloma in the European Union if the patient had previously received two unsuccessful treatments (55). Since 2006, it was also approved for use in patients with relapsed or refractory mantle-cell lymphoma (MCL) (56). In the last years, several in vitro and clinical studies have been conducted to find new additional indications of BOZ, e.g., against antibody-mediated autoimmune diseases such as myasthenia gravis and systemic lupus erythematosus (SLE) or against advanced solid malignancies such as melanoma. While BOZ could eliminate the autoantibody-producing non-neoplastic plasma cells in myasthenia gravis, it could not repair the loss of protein kinase C isoenzymes in T cells of SLE patients (57-59). In phase I studies, BOZ was found to be safe in patients with advanced solid malignancies (60).

The main biological process resulting from the inhibition of the proteasome is the stabilization of the nuclear factor kappa B (NF- κ B) pro-survival transcription factor via the inhibition of the degradation of inhibitory kappa B (I κ B) (61). Nuclear factor kappa B, when translocated to the nucleus, targets and induces multiple pro-survival anti-apoptotic genes such as (i) the caspase-8 inhibitor FLICE-inhibitory protein (FLIP), (ii) the X-linked inhibitor of apoptosis protein (XIAP) and (iii) B-cell lymphoma 2 (Bcl2) protein family members; therefore it is considered a tumor-promoting factor (62). When I κ B breakdown is inhibited due to the diminished proteasomal activity by BOZ, NF- κ B is unable to translocate to the nucleus, and therefore its downstream signaling pathways remain inactive (Figure 4) (53, 55, 61).

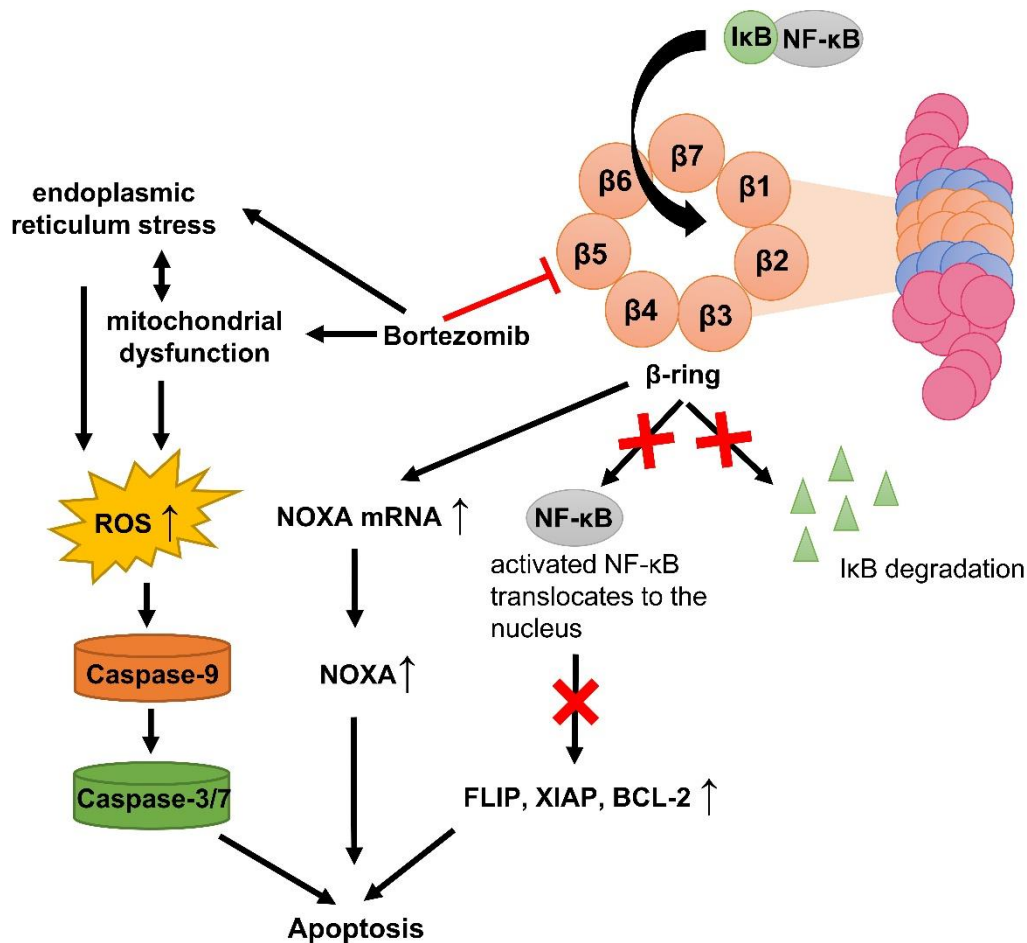


Figure 4 Mechanism of action of bortezomib (BCL-2: B-cell lymphoma 2, FLIP: the caspase-8 inhibitor FLICE-inhibitory protein, IκB: inhibitory kappa B, NF-κB: nuclear factor kappa B, ROS: reactive oxygen species, XIAP: X-linked inhibitor of apoptosis protein)

It has also been reported, that BOZ increases the expression of pro-apoptotic factors such as phorbol-12-myristate-13-acetate-induced protein 1 (NOXA) in tumor cells, whereas this effect is not observed in non-tumorous cells. This can be achieved either by stabilizing the already present NOXA protein or by enhancing the transcription of NOXA mRNA. Studies in melanoma cells show that enhancement of NOXA mRNA transcription is rather responsible for this effect of BOZ (63, 64).

Bortezomib can also induce apoptosis directly via reactive oxygen species (ROS)-mediated endoplasmic reticulum (ER) stress in head and neck squamous cell carcinoma (HNSCC) cells (65). The generated radicals damage the mitochondria, leading to caspase-9 activation (Figure 4). When the release of ROS was abolished by the superoxide

scavenger and antioxidant tiron, the apoptotic effect of BOZ was suppressed. Clinical trials also show that BOZ has a chemosensitising effect. In combination with conventional therapeutic agents such as dexamethasone or doxorubicin against previously untreated multiple myeloma, the response rate of the patients treated by the combination was higher than patients treated by the single agents (66).

Because of the increasing knowledge of its antineoplastic effects, the therapeutic regime of BOZ has developed accordingly as follows: in the treatment of multiple myeloma, it may be used as monotreatment or in combination with dexamethasone, melphalan, and prednisolone (66). For the treatment of mantle-cell lymphoma, it is typically combined with rituximab or cyclophosphamide (67).

1.3.1.2. Main side effect: bortezomib-induced peripheral neuropathy

Peripheral neuropathy refers to conditions, where the peripheral nervous system is damaged, e.g., due to (i) nutritional imbalances, (ii) infections, (iii) diabetes, or (iv) chemotherapy drugs (68). Bortezomib-induced peripheral neuropathy (BIPN) was reported in more than 30 % of patients receiving BOZ treatment for multiple myeloma (69). Due to the lack of the blood-brain barrier in the dorsal root ganglia (DRG) (70), BIPN is typically a sensory lesion in the extremities, with symptoms including paresthesia, dysesthesia, allodynia, hyperalgesia, and hypoalgesia (71). Studies found that the maximum blood concentration of BOZ correlates with the occurrence of BIPN (72, 73). All in all, the incidence of this dose-dependent side effect increases during the first 5 cycles of the treatment (74); however, the process is reversible, with symptoms decreasing and usually resolving after dose reduction or discontinuation of the treatment. Several studies discuss the pathology of BIPN, although its molecular pathology is not yet fully understood.

Among the possible pathomechanisms, insufficient ATP production caused by the damaged mitochondrial respiratory chain plays a key role. Reactive oxygen species (e.g.: superoxide anion, hydroxyl radical and hydrogen peroxide (H_2O_2)) coming from the impaired mitochondria are also generated, which can further damage the mitochondria (75). Neuronal transport dysfunction, neurotoxicity, and neurodegenerative disorders may be linked, as a large number of mitochondria can be found in the axons to supply the high energy need of the axonal transport mechanisms. It is important to optimize the quality of life of patients. Thus it is necessary to reduce the symptoms of BIPN, preferably

without reducing the anti-tumor effect of BOZ. Discontinuation or dose reduction of BOZ may be considered, but this is not optimal for tumor management (49). Other treatment options may include the use of analgesics and antidepressants (76). Furthermore, *in vitro* as well as *in vivo* studies show that antioxidant agents, e.g. N-acetyl-L-cysteine (NAC) can diminish this neurotoxic effect of BOZ and neuropathic pain was alleviated after administration of ALA (70, 77, 78). Vitamins with neuroprotective and antioxidant properties, e.g. vitamin C and vit B1 may be also effective in managing the symptoms of neuropathy (79). However, it is known from the literature that vitamin C reduces the effects of BOZ and its use is therefore not recommended (76, 80).

1.4. TIC10

TIC10 is a small-molecule drug. This type of drug is defined as chemical compounds with a molecular weight of < 900 Da. In the pharmaceutical industry, these drugs are popular, because they can be synthesized by chemical reactions, no living organisms are needed and the cost of these processes is relatively low compared to biologics (81). Thanks to their small size and simple chemical structure, they are capable to penetrate barriers like the cell membrane easily. Their physicochemical properties are well-defined and also stable. All in all, these characteristics of the small-molecule drugs result in predictable pharmacokinetics that allows them to be administered through different routes, e.g. *per os*, which is very important in improving patient adherence (82). They can target specific proteins not only extracellular but also intracellular (83). As a result, they play a significant role in diagnosing, treating, and preventing different diseases, such as tumors (84, 85).

TIC10, in the literature also known as ONC201, belongs to the group of imipridones (86). Allen and co-workers identified the molecule as a TRAIL-inducing compound during a screening of the National Cancer Institute (NCI) Diversity Set II (87, 88). Both *in vitro* as well as *in vivo* experiments showed, that TIC10 had multiple benefits over the recombinant TRAIL protein as it has aqueous solubility. Therefore they can be administered *per os*, can cross the intact blood-brain barrier, and has greater stability (87, 89, 90).

1.4.1. Mechanism of action

TIC10 can induce the transcription of the *TRAIL* gene in a p53-independent manner by the inactivation of the Akt and ERK-mediated phosphorylation of FOXO3 leading to the translocation of FOXO3 into the nucleus where it can upregulate the TRAIL mRNA (Figure 5) (91). It was also observed that TIC10 can boost the level of the TRAIL protein on the cell surface (87).

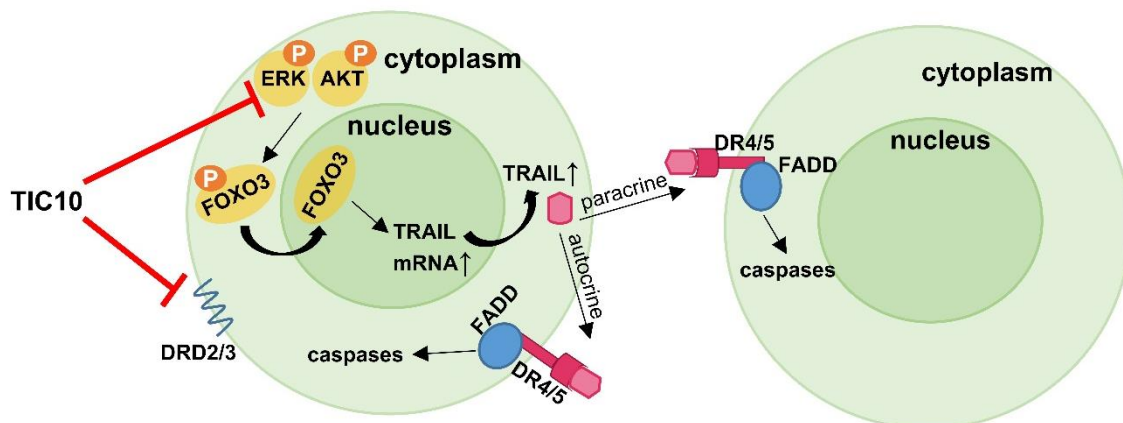


Figure 5 Mechanism of action of TIC10 (DRD2/3: G protein-coupled dopamine receptor D2/3, DR4/5: death receptor 4/5, ERK: extracellular signal-regulated kinase, FADD: Fas-associated protein with death domain, FOXO3: Forkhead box O3, TRAIL: TNF-Related Apoptosis Inducing Ligand)

TRAIL protein can auto- or paracrine engage the proapoptotic death receptor 4 (DR4) and death receptor 5 (DR5) resulting in apoptosis through the formation of Fas-associated protein with death domain (FADD) and the direct activation of the caspase cascade (89, 91). The central role of TRAIL in the mechanism of TIC10 was proved in-vivo in mice as the stable knockdown of the TRAIL protein eliminated the apoptotic effects of TIC10 (87). In the past years, a further antitumor mechanism of TIC10 has been recognized. TIC10 can activate integrated stress response in tumor cells by binding and selectively antagonizing the G protein-coupled dopamine receptor D2 (DRD2) (92, 93). As seen in the results of clinical trials, the cytotoxic effects can be detected only in tumor cells, but not in non-tumorous, healthy cells, thus the safety profile of this small molecule is very favorable (94).

2. Objectives

This Thesis aims to analyze antitumor compounds and their different combinations against the A2058 melanoma cell line.

The dissertation can be divided into two main parts. In the first part, we investigated the possible antagonistic relationship between BOZ + vit B1 or BOZ + ALA. Secondly, we screened whether TIC10 and BOZ can synergize with each other.

In detail, the following questions were posed:

1. The effect of the treatment with BOZ on A2058 melanoma cells *in vitro*.
 - a. Does BOZ have an antitumor effect against melanoma cells?
 - b. How can the neuroprotective ALA and vit B1 influence the tumor growth inhibitory effect of BOZ?
2. The effects of the TIC10 monotreatment and the binary combination of TIC10 and BOZ on A2058 melanoma cells *in vitro*.
 - a. Is the small molecule TIC10 able to impact the cell viability of the A2058 melanoma cells?
 - b. What type of interactions - additive, antagonistic or synergistic effect - occur between BOZ and TIC10?
 - c. What mechanism can be assumed in the background of the synergistic activity when used as co-treatment?

3. Methods

3.1. Cell culturing

During my projects, two different cell lines were investigated, the A2058 melanoma cell line (91100402 ECACC), that is adhesion-dependent and the U266 human myeloma cell line (85051003 ECACC), that grows in suspension. Both cell lines were purchased from the European Collection of Authenticated Cell Cultures (ECACC, Salisbury, UK).

The U266 cells, as well as the A2058 cells were cultured in RPMI 1640 medium (Sigma Ltd. St. Louis, MO, USA), that was supplemented with 10% fetale bovine serum (Invitrogen Corporation, New York, NY, USA), 2 mM L-glutamin (Invitrogen Corporation, New York, NY, USA) and 1% penicillin/streptomycin solution (Invitrogen Corporation, New York, NY, USA). In case of U266 cells, the medium was discarded in every 2nd or 3rd day and replaced with fresh one. For the subcultivation of the adherent melanoma cells, they were first washed with 0.05 M phosphate buffered saline (PBS) then resuspended by 0.25% Trypsin-EDTA solution (Sigma Ltd. St. Louis, MO, USA) and subdivided 1:3 to 1:6.

3.2. Materials

The investigated concentrations of BOZ (Velcade 3.5 mg; Janssen-Cilag GmbH, Neuss, Germany), ALA (Thiogamma 600 Injekt; Wörlag Pharma GmbH & Co.KG, Stuttgart, Germany) and vit B1 (Vitamin B1 50 mg Injection; Zentiva, Prague, Czech Republic) were selected upon the serum concentrations following a treatment (95-97). The stock solutions were dissolved in distilled water (Table 1). TIC10 (Merck/Sigma-Aldrich, Darmstadt, Germany) was dissolved in dimethyl sulfoxide (DMSO; AppliChem GmbH, Darmstadt, Germany). Due to possible photosensitivity, the stock solutions were kept in dark at low temperature (6 °C) and they were always diluted right before the experiments (Table 1.).

Table 1 Materials

Substance	Solvent	Concentration of the stock solution	The investigated concentrations
bortezomib	distilled water	3×10^{-2} M	in Results 4.1: 20, 100 and 300 ng/mL in Results 4.2: 0.5 – 121 nM via 3-fold serial dilutions
alpha-lipoic acid	distilled water	10 mg/mL	10 and 100 µg/mL
Vitamin B1	distilled water	50 mg/mL	150 and 300 nM
TIC10	dimethyl-sulfoxid	10^{-2} M	0.5 – 121 µM via 3-fold serial dilutions

3.3. Viability assays

In order to characterize the antitumor (antiproliferative) effects of the used compounds, 3 different cell viability assays were utilized, two endpoint assays (alarmarBlue and the CellTiter-Glo) and one real-time analysis (the impedance-based xCELLigence SP system). In every case, prior to the actual experiments, the utilized methods were optimized for the two different cell lines (A2058 and U266). Every test was performed in triplicates and the result was normalized to the control wells, that were only treated with medium or with DMSO (in case of TIC10).

3.3.1. alamarBlue

The alamarBlue test (Thermo Scientific, Waltham, MA, USA) contains resazurin, that can be reduced to the fluorescent resorufin upon the metabolic activity of cells. The fluorescent signal generated by the cells correlates with the number of the viable cells.

Cells were seeded in a transparent 96-well plate (10^4 cells/well) into 200 µL supplemented RPMI 1640 medium. The upcoming day, the cells were treated with the solutions of the investigated drugs. After 72h long incubation, the alamarBlue reagent was added to the wells. After 4 hours, the fluorescent signal was read by the Fluoroskan FL Microplate Fluorometer and Luminometer (excitation: 560 nm, emission: 590 nm; Thermo Scientific, Waltham, MA, USA).

3.3.2. CellTiter-Glo

The CellTiter-Glo assay (Promega, Madison, WI, USA) measures the ATP content of the metabolic active cells. Cells were seeded in a white-walled 96-well plate (10^4 cells/well; Thermo Scientific, Waltham, MA USA) into 100 μ L supplemented RPMI 1640 medium. After an overnight incubation, the cells were treated with the solutions of the investigated drugs. In the 24th or 72nd hour of the experiment, the luminescent CellTiter-Glo reagent was added to the wells. Following a 10 min long incubation, the luminescent signal was read by the Fluoroskan FL Microplate Fluorometer and Luminometer (Thermo Scientific, Waltham, MA USA).

3.3.3. Real-Time Viability Assay: xCELLigence SP

The xCELLigence SP (ACEA Biosciences, San Diego, CA, USA) device is an impedance-based system. Cells that have an intact membrane are non-conductive, they increase the impedance in an electrically conductive solution, e.g., in cell culture medium. This drop of the electron-flow can be quantified by the gold microelectrodes found in the wells of a special 96-well plate (E-plate; ACEA Biosciences, San Diego, CA, USA). This method allows us to monitor the changes in the number of the cells real-time.

First, the baseline of the cell-free medium (100 μ L/well) was registered and then the cells were added in the E-Plate into the 200 μ L/well medium (10^4 cells/well). Then, they were let to adhere overnight. Following this incubation, the cells were treated as indicated in Results and the measurement continued for the next 24-72 h. The data were registered and converted into the unitless Cell Index by the RTCA 2.0. software (Real Time Cell Analyzer; ACEA Biosciences, San Diego, CA, USA).

3.4. Quantification of interactions between drugs

Upon the results of the cell viability assays, we could define the possible synergistic, additive or antagonistic effects between the drugs by Chou-Talalay's median effect method. The calculation can be performed in the CompuSyn software (ComboSyn Inc., Paramus, NJ, US), that can be downloaded free of charge (21). The determined CI <1 , $=1$ or >1 represents synergism, additive effect or antagonism, respectively.

3.5. Apoptosis Assay

During the early phase of apoptosis, phosphatidylserine (PS) translocates to the outer membrane of the cells, while in the late phase of apoptosis the cell membrane

integrity becomes also disrupted. The Annexin V (Ax V) fluorescein isothiocyanate (FITC) conjugate (Sony Biotechnology, Weybridge, UK) has a high affinity to PS in the outer membrane, the 7-aminoactinomycin (7AAD; Sony Biotechnology, Weybridge, UK) can pass across the disrupted cell membrane and binds to DNA. The early apoptotic cells are positive for Ax V-FITC and negative for 7AAD, while both 7AAD and Ax V-FITC stain the late apoptotic/necrotic cells.

The cells were seeded in a 24-well plate (7×10^5 cells/mL). After an overnight incubation, the cells were treated as indicated. After 24-72h incubation time, the cells were harvested with TrypLE, which reagent is composed of recombinant enzyme protecting the surface proteins. After the dissociation, the cells were centrifuged, medium was discarded and replaced by 300 μ L Annexin V Binding Buffer (Sony Biotechnology, Weybridge, UK). Next, the cells were stained with Ax V-FITC and 7AAD. The fluorescence signal was detected by flow cytometer (BD FACSCalibur, Becton–Dickinson, San Jose, CA, USA) and data were evaluated by CellQuest Pro (Becton–Dickinson, San Jose, CA, USA) and Flowing 2.5.1. software (Turku Centre of Biotechnology, Turku, Finland). The results were normalized to the medium control or sample with only DMSO.

3.6. Detection of the proteasome activity

For the detection of the proteasome activity, the Cell-Based Proteasome-Glo Assay (Promega, Madison, WI, USA) was utilized. This assay enables us to specifically measure the chymotrypsin-like protease activity of the proteasome by the luminogenic proteasome substrate Suc-LLVY-aminoluciferin sequence.

Cells were seeded in a white-walled 96-well plate (A2058: 6×10^3 cells/well, U266: 10^4 cells/well; Thermo Scientific, Waltham, MA USA). The following day, the cells were treated with BOZ, ALA, vit B1 or their combinations. After 24h incubation time, the luminogenic reagent was added to the wells. The generated luminescence was detected by the Fluoroskan FL Microplate Fluorometer and Luminometer (Thermo Scientific, Waltham, MA USA). The value of the luminescent signal of the sample blank was subtracted from all wells before data analysis. The raw data were normalized to the control.

3.7. Luminescence-based measurement of intracellular H₂O₂ levels

The ROS-Glo H₂O₂ cell-based assay (Promega, Madison, WI, USA) was performed to measure the intracellular H₂O₂ level post BOZ, ALA or combination treatments. This assay contains a H₂O₂ substrate, that can be transformed into a luciferin precursor by the generated H₂O₂. In the consecutive step the luciferin precursor can be converted to luciferin, that produces light signal.

Cells were seeded in a white-walled 96-well plate (10⁴ cells/well; Thermo Scientific, Waltham, MA USA). After 24h of culturing, the cells were treated with BOZ, ALA, vit B1 or their combinations and incubated for 24h. Prior to the end of the incubation time, the H₂O₂ substrate was added to the wells and the plate was further incubated for 6h. Finally, the luciferin detection reagent is added to the wells. The luminescent measurements were performed using the Fluoroskan FL Microplate Fluorometer and Luminometer (Thermo Scientific, Waltham, MA USA). The value of the luminescent signal of the sample blank was subtracted from all wells before data analysis. The raw data were normalized to the control.

3.8. Microscopic detection of intracellular ROS levels

To quantitate cellular oxidative stress of the A2058 adherent cells, we used the CellROX Deep Red fluorescent dye (Thermo Scientific, Waltham, MA USA). This fluorogenic probe is non-fluorescent in reduced state, but it exhibits fluorescence when oxidized by ROS.

To reduce the background signals and crosstalk between the wells, the cells were plated in a 96-well black-walled plate (10⁴ cells/well/100 μ L; (Greiner Bio One, Frickenhausen, Germany). After an overnight incubation, the cells were treated with BOZ, ALA, their co-treatments. The ROS scavenger NAC as negative control was used, too. N-acetyl-l-cysteine is a thiol, that has direct and also indirect antioxidant properties, e.g., it increases the level of cysteine that plays a crucial role by the regeneration of glutathione (98, 99). Following the 24h long incubation time, the CellROX Deep Red reagent was added to the wells (final concentration: 5 μ M). To be able to compare the results, a nuclear stain, Hoechst 33342, was also utilized (final concentration: 0.5 μ g/mL; (Thermo Scientific, Waltham, MA USA). After a 30 min long incubation, the cells were washed two times with PBS and then fixed with 3.7% formaldehyde. Images were taken by Celldiscoverer 7 system using 5 \times Plan-Apochromat λ /0.35 NA objective with 2 \times tube

lens (Carl Zeiss AG, Jena, Germany). Intensity values of the red channel, that represents intracellular ROS, were normalized to the blue channel, that represents the cell nuclei. The images were analyzed by ImageJ software (NIH, USA).

3.9. Proteome profiler human apoptosis array kit

For the detection of 35 apoptosis-related proteins, a membran-based sandwich immunoassay was conducted (Human Apoptosis Array Kit, R&D Systems, Minneapolis, MN, USA).

Cells (2×10^6 cells/flask) were treated with BOZ 20 ng/mL, ALA 100 μ g/mL and their combination. Following the 24h incubation, they were harvested with TrypLE (Thermo Fisher Scientific, Waltham, MA, USA) and then centrifuged (1,000 g; 5min). The supernatant was removed and collected, while the cell pellet was washed with PBS and then extracted with Lysis Buffer 17 of the assay. From the supernatant, the apoptotic bodies were also separated by centrifugation (2,500 g; 15min; 4°C). Then this pellet was also extracted with Lysis Buffer 17. The two kinds of lysates were mixed and then total protein quantity was measured in all treatment groups by the colorimetric BCA assay (Thermo Scientific, Waltham, MA USA).

The membrane-based assays were loaded with 225 μ g proteins/membrane. The test was conducted in accordance with the manufacturer's instructions. The membranes were visualized by Bio-Rad Chemidoc XRS + system. The intensity of the proteins spots were evaluated by Image Lab Software (BIO-RAD, USA). The protein level of the treated samples was normalized to the untreated medium control sample.

3.10. Flow Cytometric Detection of Death Receptors

The expression of the cell surface-bound DR4 and DR5 was measured by flow cytometry.

Cells (10^5 cells/mL) were cultured in a 12-well plate and treated as indicated. Then the cells were harvested with Tryple reagent (Thermo Fisher Scientific, Waltham, MA, USA) and washed with PBS. The supernatants were discarded and the pellets were resuspended in 250 μ L PBS. The samples were incubated either with phycoerythrin conjugated isotype control, phycoerythrin conjugated anti-DR4 antibody or phycoerythrin conjugated anti-DR5 antibody (Sony Biotechnology, Weybridge, UK). To reduce the background noise, the cells were centrifuged again (5min, 1200 rpm) and resuspended in 300 μ L PBS. The

measurements were done by BD FACSCalibur flow cytometer (BD FACSCalibur, Becton–Dickinson, San Jose, CA, USA). The data analysis was performed in Flowing 2.5.1. software (Turku Centre of Biotechnology, Turku, Finland). The surface expression of DR4/DR5 on the the treated cells was normalized to the untreated medium control sample.

3.11. Statistical analysis

The results were evaluated by MS Excel and OriginPro 8.0 software. The data are presented as mean \pm standard deviation (SD). For statistical analysis, the one-way analysis of variance (ANOVA) followed by Fisher's least significant difference (Fisher's LSD) post hoc test was performed. The IC₅₀ value were determined by fitting a sigmoidal dose-response curve to the data using Origin Pro 8.0. Treated samples were compared to the medium control or in case of TIC10 to DMSO control. The levels of significance are shown as follows: x: $P < 0.05$; y: $P < 0.01$; z: $P < 0.001$.

4. Results

4.1. The impact of alpha-lipoic acid and vitamin B1 on the antitumor effects of bortezomib

In the following chapter, we would like to discuss the possible interactions and how two neuroprotective vitamins (ALA, vit B1) may decrease the antitumor effect of BOZ. Two cell lines were investigated, the U266 multiple myeloma cell line as a reference and the A2058 metastatic melanoma cell line. As in the last years, BOZ seemed to have a partial response efficacy against solid tumors as a single agent as well as in combination with other chemotherapeutic agents (100-102). The tested concentrations (BOZ: 20, 100, 300 ng/mL; ALA: 10, 100 µg/mL and vit B1: 150, 300 nM) were chosen based on their maximal plasma concentrations that occur after the clinical use (95, 97, 103).

4.1.1. The anti-proliferative effect of bortezomib is decreased by alpha-lipoic acid

To determine the potency of BOZ against the U266 myeloma and the A2058 melanoma cell lines, the half-maximal inhibitory concentration (IC_{50}) in the 24th hour of the treatment was measured. The results show, that the myeloma cells were more sensitive to BOZ compared to the melanoma cells (2.17 nM vs. 158 nM, respectively) (Figure 6 A-B).

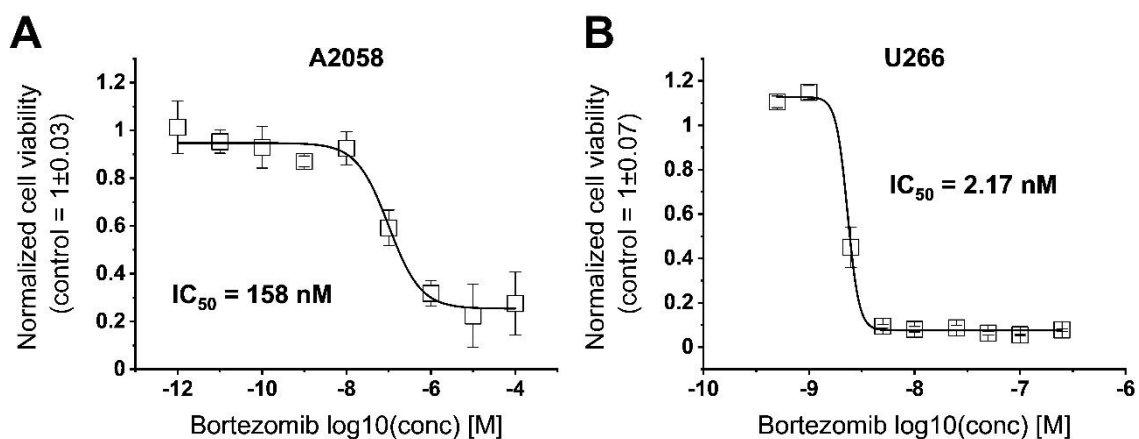


Figure 6 U266 myeloma cells are more sensitive to bortezomib (BOZ). Concentration-response curves for A2058 (A) and U266 (B) cells treated with BOZ for 24h. The data are normalized to the control wells. Data are given as mean values \pm SD (n=3).

In the upcoming experiments, the binary combinations of BOZ + ALA or BOZ + vit B1 were tested aiming to determine combinations where the neuroprotective vitamins can counteract the effect of BOZ compared to the only-BOZ treated cells (Figure 7 A-B). As can be seen from the results, the tested BOZ concentrations (20, 100, and 300 ng/mL) were effective against both cell lines. In the case of the A2058 cells, concentration dependence was observed (Figure 7 A). There was one case where the decrease in the antitumor effect of BOZ against the A2058 cell line could be detected, and 100 µg/mL ALA could reduce the effect of 20 ng/mL BOZ. The antioxidant ALA and vit B1 were also tested on their own, whether they could influence the cell viability of these cell lines. Surprisingly, the lower concentration of ALA had an impact on the myeloma cells, although there were no significant differences compared to the control (Figure 7 C-D).

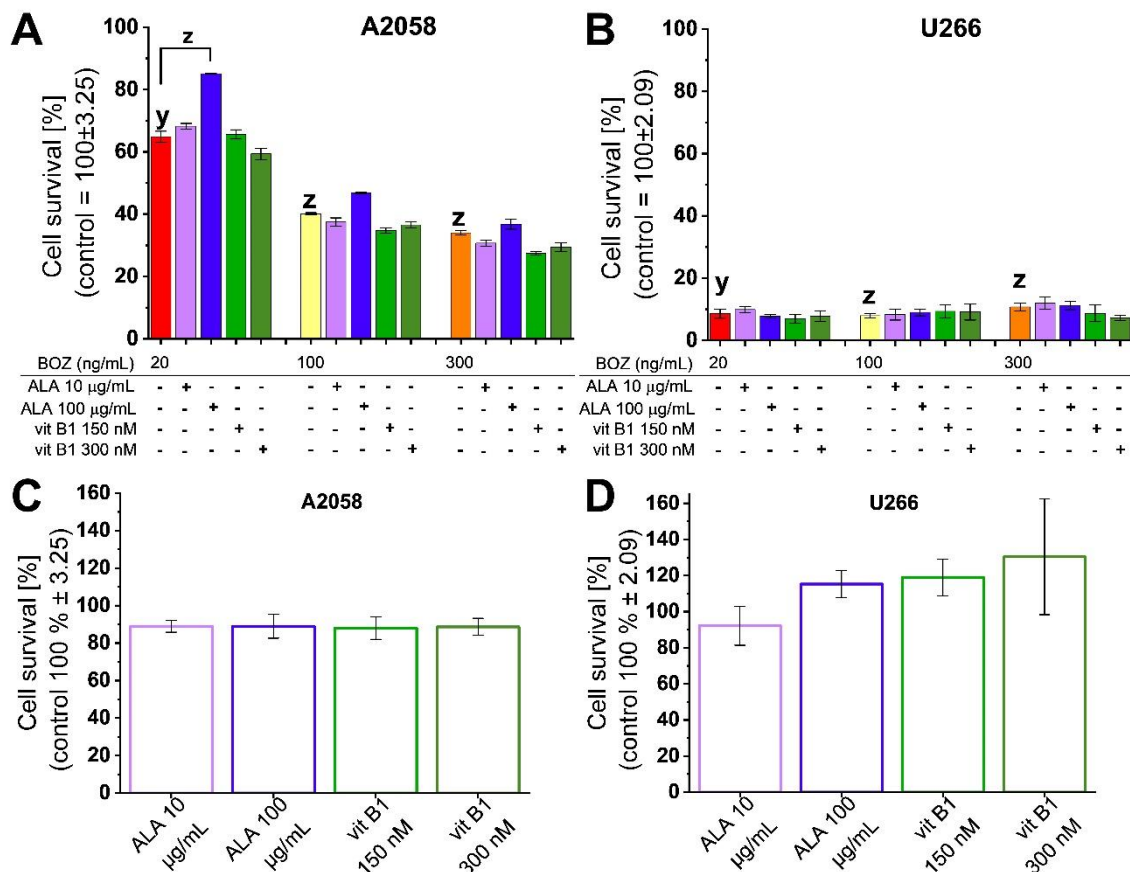


Figure 7 Alpha-lipoic acid (ALA) counteracted the anti-proliferative effect of bortezomib (BOZ) on melanoma cells. Influence of ALA and vitamin B1 (vit B1) on bortezomib-mediated cell death on A2058 performed by xCELLigence SP (A) and U266 cells performed by CellTiter-Glo Luminescent assay (B) and as monotreatments on

A2058 (C) and U266 cells (D) after 24h incubation. Data are given as mean values \pm SD ($n = 3$). The levels of significance are shown as follows: x : $P < 0.05$; y : $P < 0.01$; z : $P < 0.001$.

To validate these results, a combination analysis of BOZ + ALA was performed in the CompuSyn Software that works based on Chou-Talalay's Combination Index Theorem. A strong antagonism was found between 20 ng/mL BOZ and 100 μ g/mL ALA (CI = 8.67) (Figure 8 A-B).

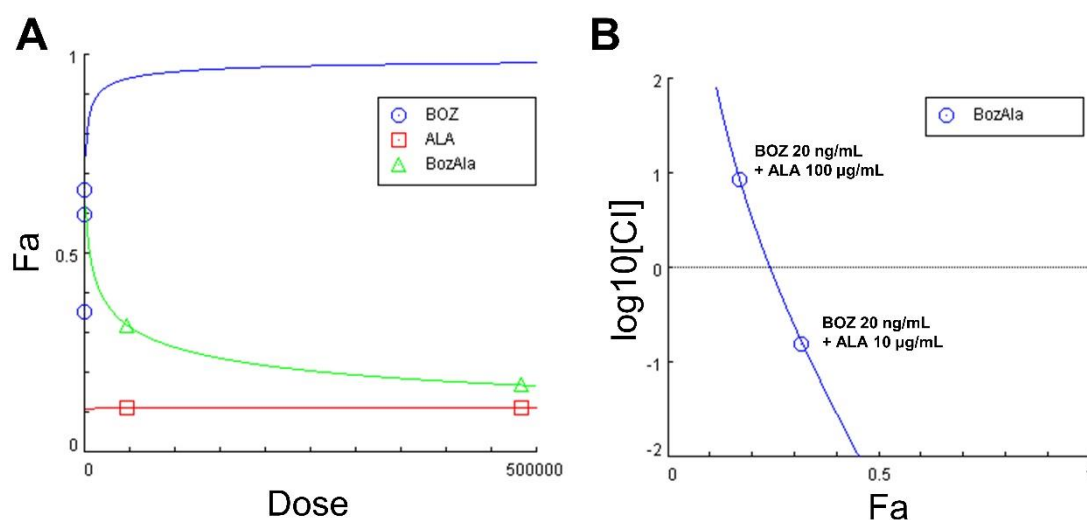


Figure 8 The antagonism between alpha-lipoic acid (ALA) and bortezomib (BOZ) on melanoma cells. The dose-effect plot on A2058 cells following 24h of treatment with BOZ, ALA, and their combination (BozAla) (A) depicted by CompuSyn Software. Logarithmic combination index plot (B) for BOZ (20 ng/mL) + ALA (10-100 μ g/mL) co-treatments are plotted. Data was obtained via CompuSyn analysis. CI: combination index; Fa: fraction affected

Apoptosis was studied by the Ax V assay. The BOZ monotreatment induced a major increase in the percentage of Ax V positive cells. Both antioxidants were able to impact the apoptotic effects of BOZ (Figure 9 A-B). Moreover, an increase in the number of the Ax V positive cells was detected in many instances: e.g., (i) A2058 cell: 100 ng/mL BOZ + 100 μ g/mL ALA or 300 nM vit B1; (ii) U266 cell: 20, 100, 300 ng/mL BOZ + 10 or 100 μ g/mL ALA, respectively. Unexpectedly, no significant decrease could be observed in the 20 ng/mL BOZ + 100 μ g/mL ALA combination, which combination was proved to be antagonistic in viability measurements, compared to the 20 ng/mL BOZ-

treated cells. In monotreatments, both 100 $\mu\text{g/mL}$ ALA and 300 nM vit B1 could induce apoptosis (Figure 9 C-D), but this effect was much smaller than in case of BOZ.

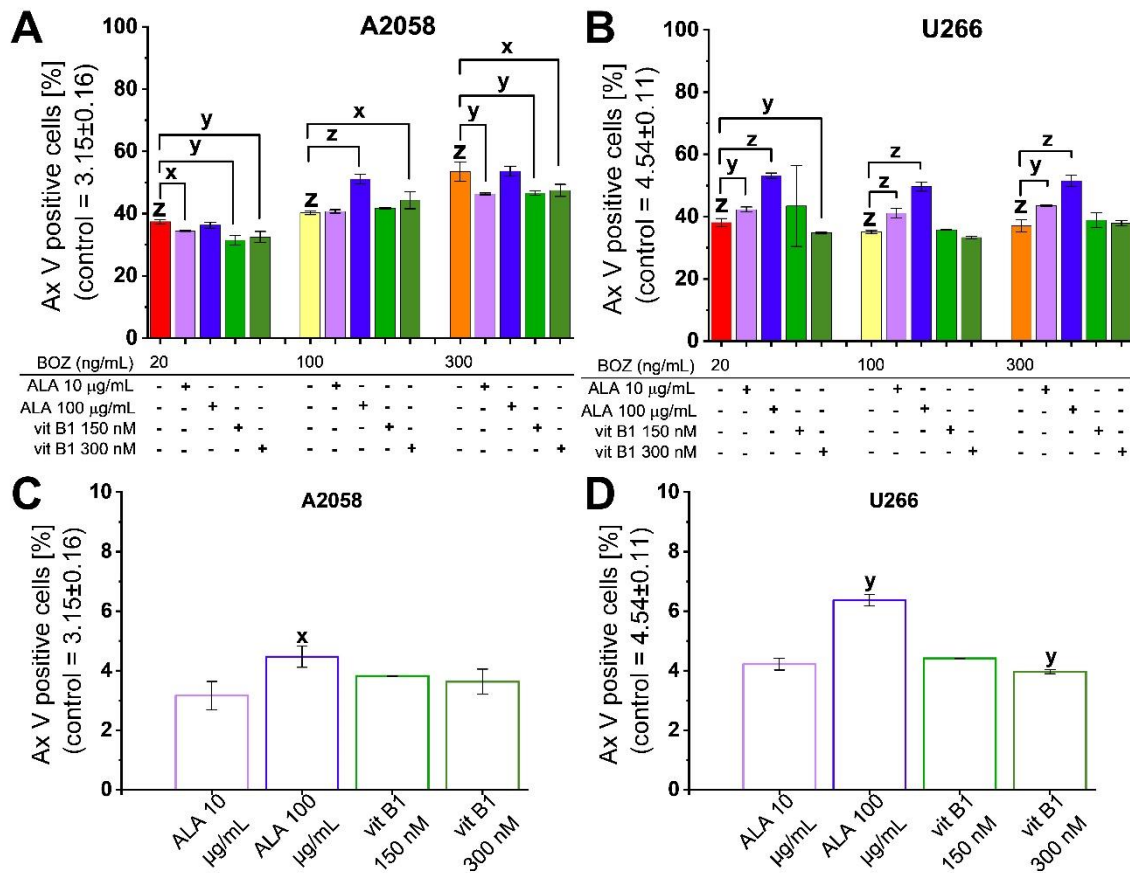


Figure 9 Bortezomib (BOZ) increased the percentage of the early apoptotic (Annexin V - Ax V - positive) cells, that effect was slightly altered by the co-treatments with alpha-lipoic acid (ALA) or vitamin B1 (vit B1) in A2058 (A) and U266 (B) cells after 24h long incubation. Apoptosis in A2058 (C) and U266 (D) cells treated with single 10 or 100 $\mu\text{g/mL}$ ALA, and 150 or 300 nM vit B1 for 24h long was analyzed by Ax V assay. Data are given as mean values \pm SD ($n = 2$). The levels of significance are shown as follows: x: $P < 0.05$; y: $P < 0.01$; z: $P < 0.001$.

4.1.2. The increase in the proteasome activity following co-treatment with ALA + BOZ 20 ng/mL is concentration-dependent

Regarding the pharmacodynamics of BOZ, we hypothesized, that ALA could impact the proteasome-inhibiting effect of BOZ. Before testing the combinations on the chymotrypsin-like activity of the proteasome, the IC_{50} value of BOZ was quantified on both cell lines after 24h incubation (Figure 10 A-B). The A2058 cells were slightly less

sensitive to BOZ ($IC_{50} = 4.39$ nM, Figure 10 A) than the U266 cells ($IC_{50} = 1.49$ nM, Figure 10 B). This result is in accordance with the cell viability results.

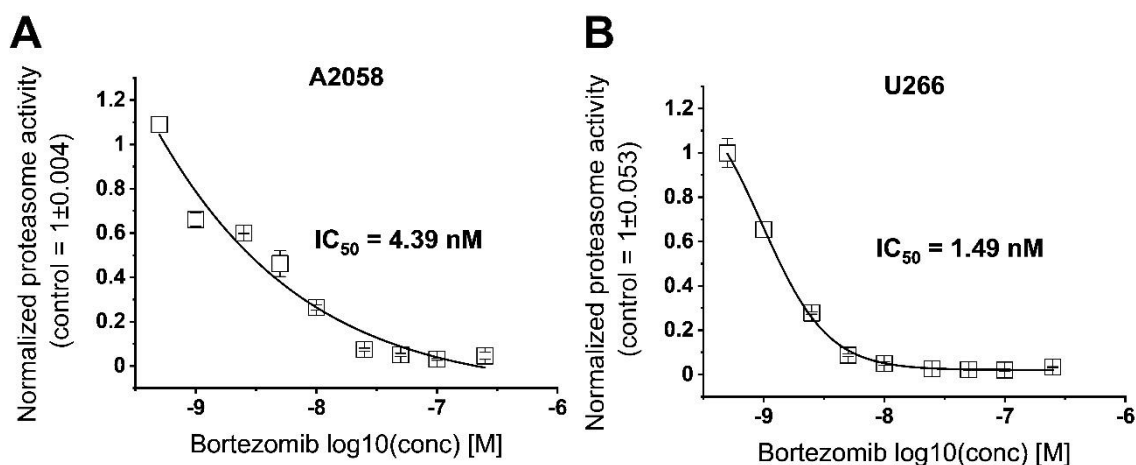


Figure 10 A2058 was less sensitive to the proteasome inhibiting effect of bortezomib (BOZ) than U266 cells. Dose-response curves and IC_{50} values of BOZ treatment (concentration range: 10^{-9} - $10^{-6.5}$ M, 24h) on the proteasome activity in melanoma A2058 (A) and myeloma U266 (B) cells. The data were normalized to the control wells. Data are given as mean values \pm SD ($n = 3$).

In cases where the single concentrations of BOZ were tested, a drastic drop could be seen in the activity of the proteasome (Figure 11 A-B). However, no concentration dependence is noticeable. The antioxidants could not affect the proteasomal chymotrypsin-like activity alone (Figure 11 C-D). They could barely antagonize BOZ, but only the co-treatment with 100 $\mu\text{g/mL}$ ALA was able to modify the effects of 20 ng/mL BOZ in A2058 cells. In this case, a significant increase was noticeable (Figure 11 A). That result is also in line with the outcomes of the cell viability experiments.

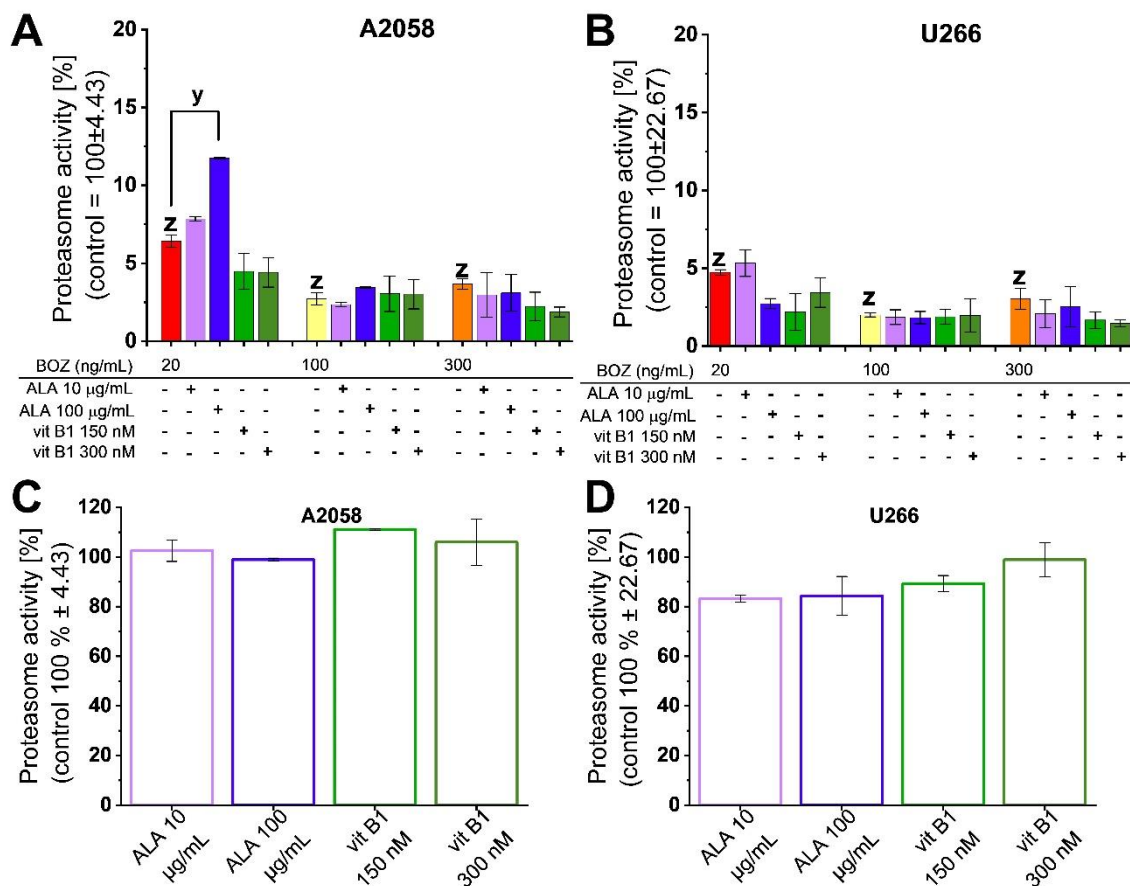


Figure 11 Alpha-lipoic acid (ALA) could antagonize proteasome inhibiting effect of bortezomib (BOZ). The effect of BOZ and its combinations with antioxidants on the chymotrypsin-like activity of the proteasome in A2058 (A) and U266 (B) cells. The effect of 10 or 100 μ g/mL ALA and 150 or 300 nM vitamin B1 (vit B1) on the chymotrypsin-like activity of the proteasome in A2058 (C) and U266 (D) cells. Cells were treated with therapeutic agents as indicated for 24h. The data were normalized to the control wells. Data are given as mean values \pm SD ($n = 3$). The levels of significance are shown as follows: x: $P < 0.05$; y: $P < 0.01$; z: $P < 0.001$.

4.1.3. Oxidative status changes after treatment with bortezomib and alpha-lipoic acid compared to the bortezomib treatment

We presumed, that because of the antioxidative properties of ALA and vit B1, they could have an impact on the pro-oxidative properties of BOZ. Thus, with the help of a luminescence-based assay, the H_2O_2 level of the A2058 and U266 cells was tested. The results show, that the quantity of H_2O_2 was higher only in the BOZ-treated myeloma cells (Figure 12 A-B). The two antioxidants could not mitigate the H_2O_2 -inducing effect of

BOZ in the U266 cell line, while in the A2058 cells, 100 $\mu\text{g/mL}$ ALA could markedly reduce the amount of H_2O_2 compared to those treated with 20 ng/ml BOZ (Figure 12 C-D).

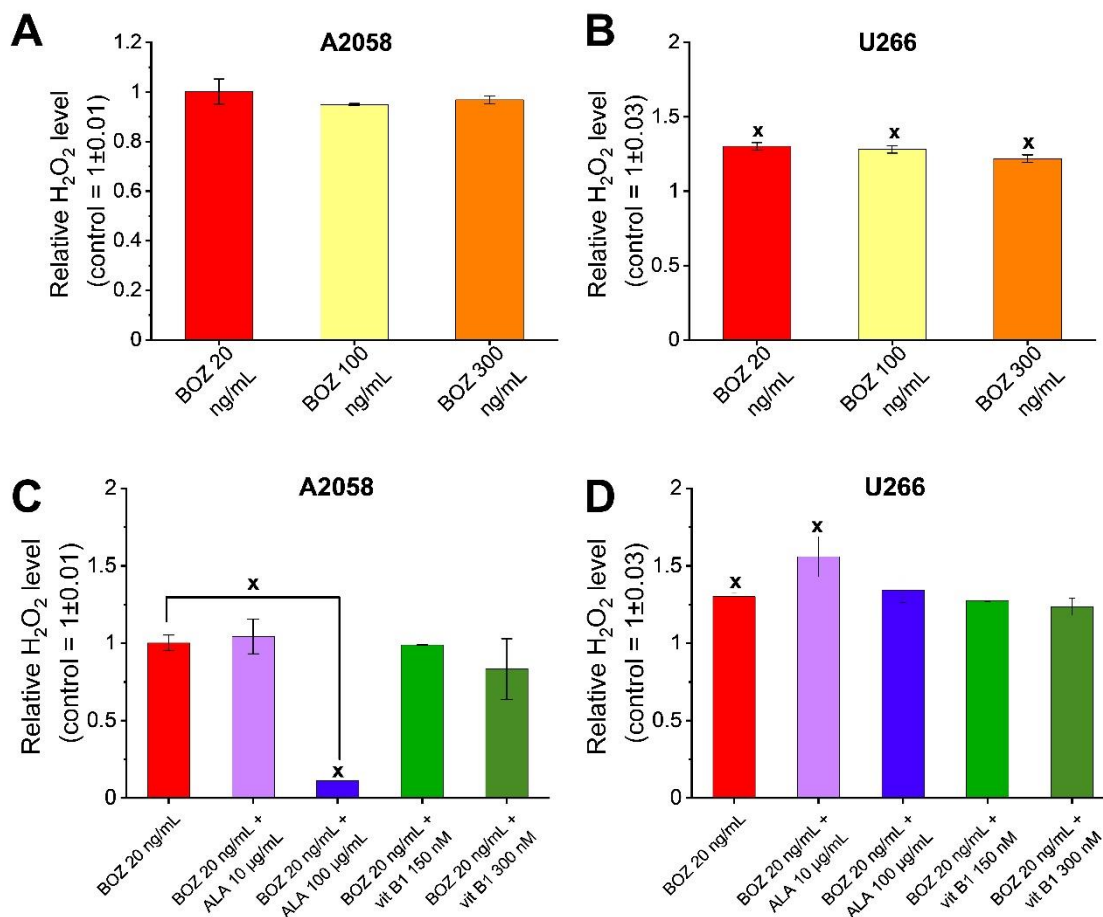


Figure 12 Bortezomib (BOZ) and alpha-lipoic acid (ALA) co-treatment markedly reduce the relative H_2O_2 status in A2058 cells. The relative H_2O_2 level of the cells was determined in A2058 (A, C) and U266 (B, D) cells after 24h long incubation with 20, 100, and 300 ng/mL BOZ (A, B) and combinations of 20 ng/mL BOZ + 10 or 100 $\mu\text{g/mL}$ ALA and 150 or 300 nM vitamin B1 (vit B1) (C, D). Data are given as mean values \pm SD ($n = 2$). The levels of significance are shown as follows: x: $P < 0$.

With the automated high-throughput Celldiscoverer 7 microscope, the oxidative status of the adherent A2058 melanoma cells stained by CellROX Deep Red could be quantified. To be able to normalize the intensity of the red channel to the number of viable cells, the Hoechst 33342 nucleus fluorescent staining was also performed. Regarding these microscopic results, BOZ caused an increase in the red channel in every investigated

concentration, indicating the formation of ROS. However, this effect of BOZ did not depend on the concentration (Figure 13.).

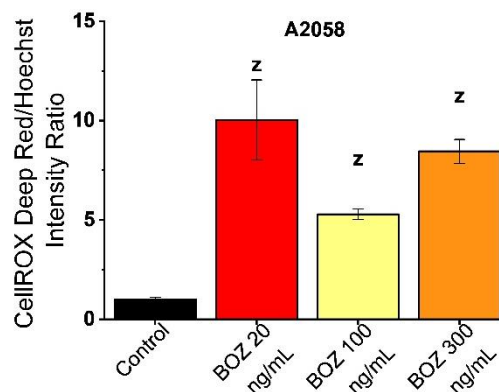


Figure 13 Bortezomib (BOZ) induced oxidative stress in melanoma cells. A comparison of the intensity values of the red channel normalized to the cell nuclei is shown. The cells were imaged on Zeiss Celldiscoverer 7 using $10\times$ magnification. Melanoma cells were treated as indicated for 24h. Data in duplicates were expressed as mean \pm SD. The level of significance is shown as follows: z: $P < 0.001$.

Contrary to certain expectations neither 10 nor 100 $\mu\text{g/mL}$ ALA was able to show its impact in this experiment. They could not alter the results of BOZ (Figure 14 A-B). To validate the pro-oxidative property of BOZ a negative control, NAC (1000 μM) was also utilized. Figures 14 A-B show, that the ROS-formation effect of BOZ (20 ng/mL) could be neutralized by adding 1000 μM NAC.

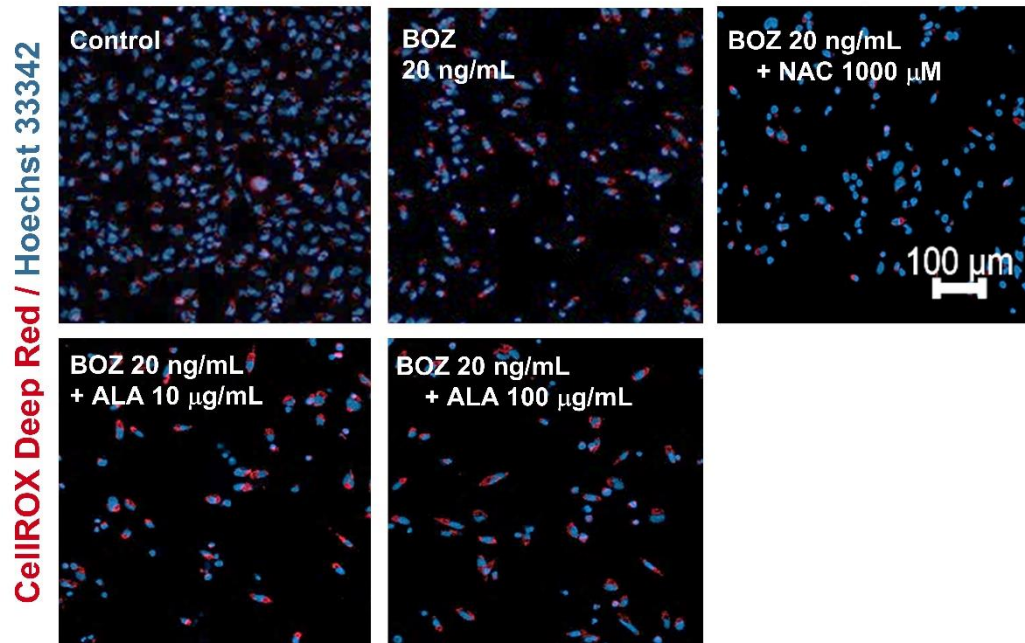
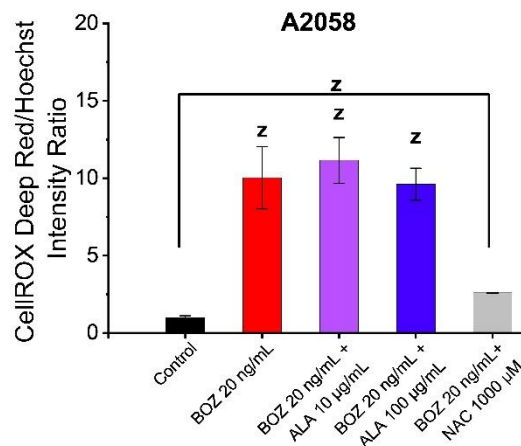
A**B**

Figure 14 Alpha-lipoic acid (ALA) did not change the oxidative status of the melanoma cells treated with bortezomib (BOZ). The cells were imaged on Zeiss Celldiscoverer 7 using $10\times$ magnification. Melanoma cells were treated as indicated for 24h. (A) A comparison of the intensity values of the red channel normalized to the cell nuclei is shown. (B) Data in duplicates were expressed as mean \pm SD. N-acetyl-L-cysteine (NAC) served as a negative control. The level of significance is shown as follows: z: $P < 0.001$.

4.1.4. The loss of the antitumor effect may be mediated by the altered levels of apoptotic proteins

To investigate the role of the apoptotic proteins in the proven loss of efficacy of 20 ng/mL BOZ against the melanoma cells in combination with 100 µg/mL ALA, we performed a semi-quantitative analysis of 35 apoptosis-related proteins.

Figure 15 highlights the results of 20 ng/mL BOZ, 100 µg/mL ALA, and their co-treatment on A2058 melanoma and U266 myeloma cells. The relative protein levels (fold change) are presented in Figure 15 BOZ could activate different apoptosis-related proteins in the two cell lines (Figure 15 A-B). In the myeloma cell line, BOZ caused an increase in the expression of two heat shock proteins (Hsp70 and Hsp60), the heme oxygenase 1 (HO-1), and the cleaved caspase-3 proteins (Figure 15 B). In the melanoma cells treated with BOZ (20 ng/mL), an increase of HO-1 and cleaved caspase-3 was also detectable along with the activation of claspin. No Hsp70 or Hsp60 activation could be found.

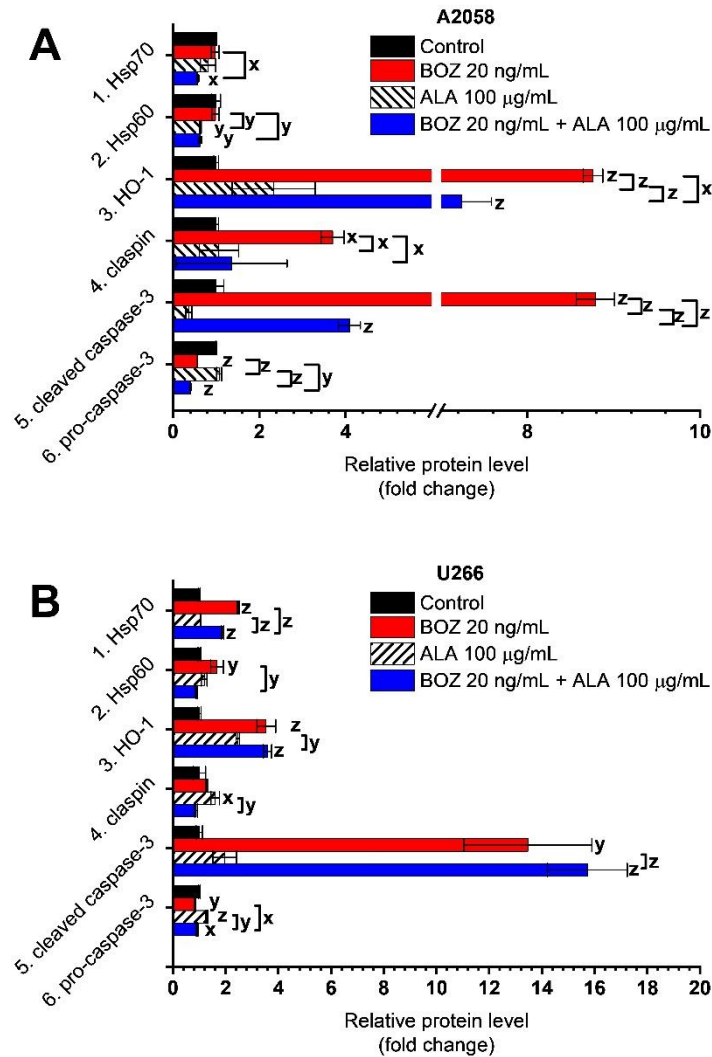


Figure 15 Co-treatment of 20 ng/mL bortezomib (BOZ) with 100 µg/mL alpha-lipoic acid (ALA) alters the apoptotic proteome profile in melanoma cells. Semi-quantitative proteomic profiling of A2058 (A) and U266 (B) cells after being treated with 20 ng/mL BOZ, 100 µg/mL ALA, and their combination for 24h. The levels of significance are shown as follows: x: $P < 0.05$; y: $P < 0.01$; z: $P < 0.001$.

After the treatment with the combination of 20 ng/mL BOZ + 100 µg/mL ALA, 6 proteins – Hsp70, Hsp60, HO-1, caspin, cleaved caspase-3, pro-caspase-3 – were found which had a significantly different level in the co-treated cells compared to the BOZ-treated cells. In the co-treated melanoma cells, we observed a decrease in the amount of HO-1, caspin, and cleaved-caspase-3 compared to the BOZ treatment (Figure 15 A). These changes in protein expression were not seen in the myeloma cells (Figure 15 B).

4.2. The effects of the combinatorial treatment of TIC10 and bortezomib

In the second part of the thesis, we aimed to define combinations of BOZ and TIC10 (also called ONC201), where the co-treatments have higher efficacy than the matching monotreatments.

4.2.1. TIC10 has no IC₅₀ value on A2058 melanoma cells

Between 2017-2021, the Chemotaxis Research Group (head: Prof. László Kőhidai) took part in the National Competitiveness and Excellence Program (NVKP_16-1-2016-0036), where more than 400 new, possibly antitumor molecules were tested on 4 different cell lines (PANC1, human pancreatic carcinoma of ductal origin; COLO205, human colon adenocarcinoma; A2058, human malignant melanoma with high invasiveness and EBC1, human lung squamous cell carcinoma). A large portion of the molecules was synthesized by the group of Dr. Antal Csámpai (Department of Organic Chemistry, Eötvös Lóránd University).

In this research, TIC10 was one of the reference molecules and its antiproliferative effects were tested by alamarBlue assay on A2058, COLO 205, and EBC1 cells, and by the real-time xCELLigence assay on PANC1 cells after 72h long incubation time. We have found, that TIC10 had an IC₅₀ value on PANC1, COLO205, and EBC1 cells (1.7 ± 0.3 μ M, 5.0 ± 2.9 μ M, and 7.0 ± 0.5 μ M, respectively), but no IC₅₀ value could be determined on A2058 cells (>25 μ M) in the tested concentration range (104).

4.2.2. Bortezomib and TIC10 were more effective together than the matching monotreatments in A2058 cells

First, an end-point viability assay was performed after 72h long incubation with A2058 as well as with U266 cells (Figure 16 A-B). The investigated concentrations for BOZ were 0.5 – 121 nM, and for TIC10 0.5 – 121 μ M via 3-fold serial dilutions. The investigated concentrations of BOZ are clearly lower than the IC₅₀ value after 24h incubation (A2058: 158 nM, U266: 2.17 nM). Since in the preliminary experiments we could observe that the TIC10 elicited its antitumor effect in long-term manner, we aimed to study the effects of the combinatory treatments long-term, thus these subtoxic doses of BOZ were utilized (Figure 16 A-B). For better understanding, the data are presented in heatmaps. We have found, that 1.5 nM BOZ or 1.5 μ M TIC10 were already able to kill

more than 50 % of the U266 myeloma cells, however against A2058 melanoma cells, these concentrations remained ineffective.

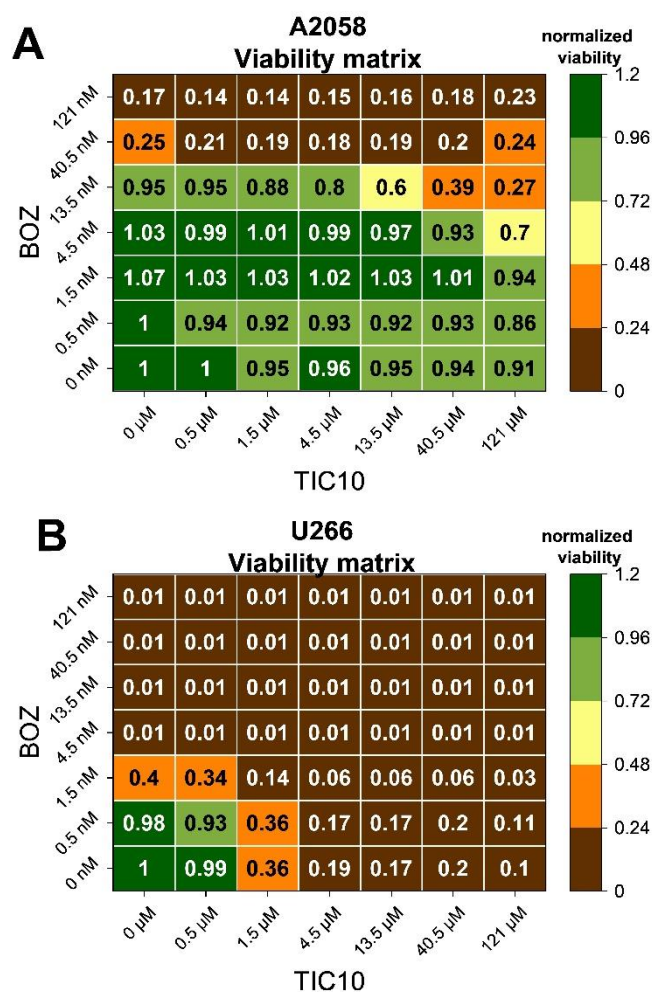


Figure 16 Bortezomib (BOZ) and TIC10 co-treatments were more effective than the matching monotreatments in A2058 cells. Heatmaps showing antiproliferative effects of BOZ, TIC10 and their combinations on A2058 (A) and U266 (B) cells after 72h of incubation. Normalized viability data are expressed as a ratio of medium control. Data are presented as mean values ($n = 3$).

In the case of the melanoma cells, TIC10 had no remarkable effect alone, and only two concentrations of BOZ, 40.5 and 121 nM were able to reduce more than 50% of the viable cells (Table 2).

Table 2 Comparison of IC₅₀ values of bortezomib and TIC10 on A2058 and on U266 cells after 72h

drug	A2058	U266
bortezomib	23.07 ± 2.41 nM	1.45 ± 0.06 nM
TIC10	ND	0.97 ± 0.26 μM

The data are normalized to the control wells. Data are given as mean values ± SD (n=3). The IC₅₀ value of BOZ was determined by fitting a sigmoidal dose-response curve to the data using Origin Pro 8.0.

Figure 17 shows Chou-Talalay's method calculated Combination index values for the A2058 melanoma cells. Synergism is detected when the Combination index is less than 1. To reduce the number of possible combinations in the further experiments, three criteria were set up: (i) where the decrease in the cell viability was around 50% or more compared to the matching monotreatments, (ii) where the concentrations of the single agents were as low as possible and (iii) where the DMSO (solvent of TIC10) was under 0.5 v/v%, due to the possible cytotoxic effects of this solvent (105). Two combinations were found for further analysis: 13.5 nM BOZ + 40.5 μM TIC10 and 13.5 nM BOZ + 13.5 μM TIC10 (CI = 0.25 and 0.33, respectively). Due to the high response rate of U266 against BOZ, in the following experiments, only the A2058 cell line was investigated.

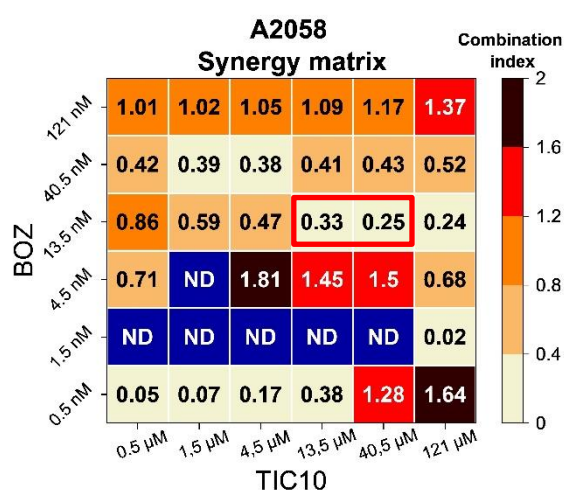


Figure 17 Strong synergism between bortezomib (BOZ) and TIC10 was detected in A2058 cells. Heatmaps showing the combination index values of BOZ, TIC10, and their combinations on A2058 after 72h of incubation. The combination index < 1, = 1,

or > 1 represents synergism, additive effect, or antagonism, respectively. ND: not detectable.

To validate the results of the endpoint assay, a real-time, impedance-based, cell viability assay was performed. After a 24h long incubation time, the plated cells were treated with medium, DMSO, 13.5 nM BOZ, 13.5 and 40.5 μ M TIC10, 13.5 nM BOZ + 40.5 μ M TIC10, and 13.5 nM BOZ + 13.5 μ M TIC10 (Figure 18). The antitumor effect of BOZ evolved immediately after the treatment, as the cells could not proliferate in the next 36h (Figure 18 A). Interestingly, this long-term experiment drew attention to the possible loss of sensitivity against antitumor drugs, as the melanoma cells could start to proliferate after 36h-long treatment despite the presence of BOZ (Figure 18 B). The opposite was seen with the TIC10 agent, first, the cells were not affected, but after 48h the number of viable cells started to decrease. When treated with the co-treatments, the two different drugs together could achieve a greater and long-term (for 72h) cytotoxic effect compared to both monotreatments (Figure 18 C).

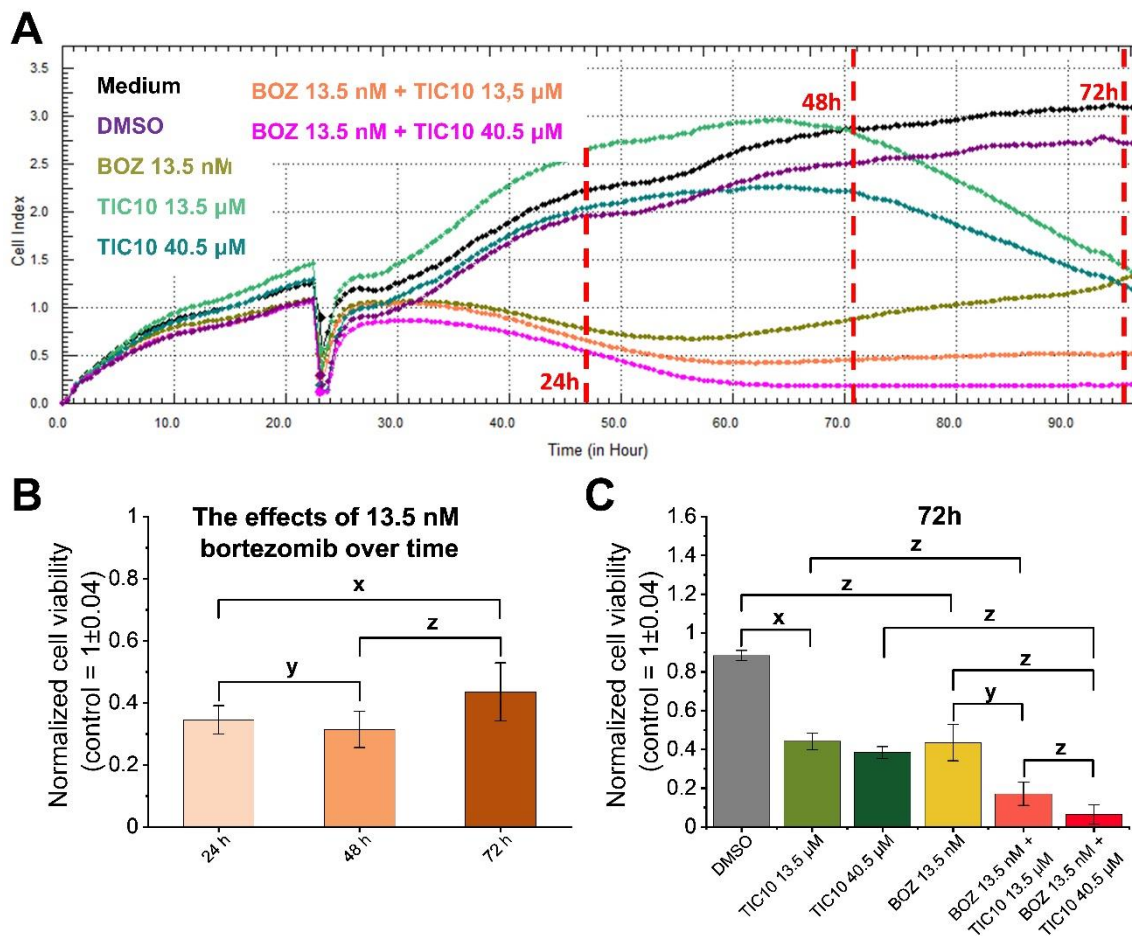


Figure 18 Bortezomib (BOZ) and TIC10 co-treatments could achieve a greater and long-term (for 72h) cytotoxic effect compared to both monotreatments. Raw data of the real-time analysis of cell viability after 13.5 nM BOZ, 13.5 and 40.5 μ M TIC10, and their co-treatments (A). Cell Index, a relative and dimensionless value, represents the impedance changing due to cell adhesion, spreading (0-24h measurement interval), and then cell viability decreasing effect of the treatments (24-72h measurement interval). Data are represented as mean values ($n=3$). Column charts representing the cell viability at different time points of BOZ treatments (B) and after 72h treatments with the combinations (C). The data were normalized to the medium control. Data are presented as mean values \pm SD ($n = 3$). The levels of significance are shown as follows: $x: p < 0.05$; $y: p < 0.01$; $z: p < 0.001$.

As the most significant effects of the co-treatments were registered after 72h, the Ax V and 7AAD assays were also performed after 72h to see the percentages of the early and late apoptotic cell populations. The percentage of the early apoptotic (only-Ax V positive)

cells was only slightly increased by the mono- or co-treatments with BOZ (Figure 19 A) and cells were rather found in the late apoptotic stage (Ax V/7AAD double-positive cells) compared to the controls (Figure 19 B). Similarly to the cell viability results, both co-treatments led to an increase in the number of late-apoptotic cells in a dose-dependent manner compared to the monotreated cells.

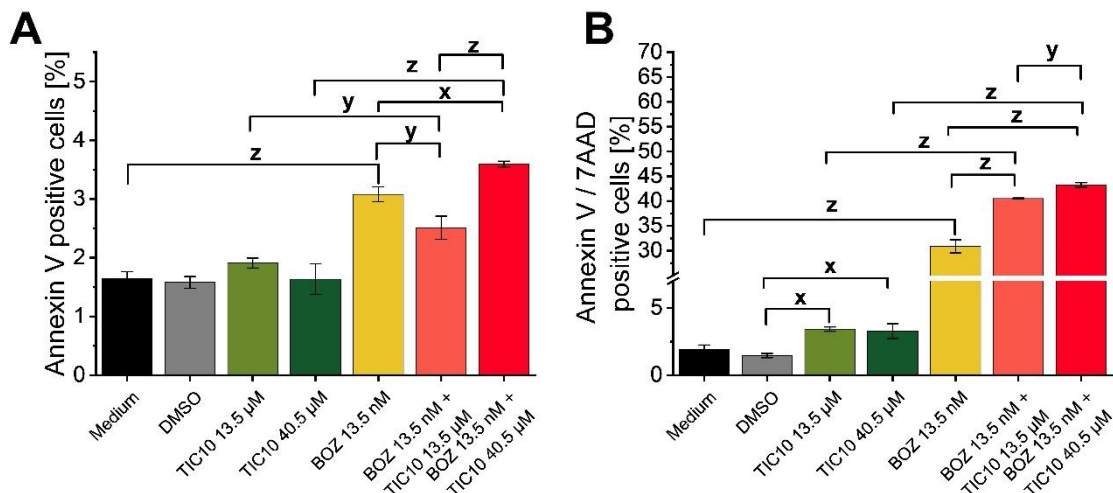


Figure 19 The number of Annexin V (Ax V) and 7AAD positive melanoma cells was higher after both co-treatments compared to the monotreatments. Percentage of early apoptotic (Ax V-positive) (A) and late apoptotic (Ax V and 7AAD double-positive) (B) cells after 72h treatment with 13.5 nM bortezomib (BOZ), 13.5 and 40.5 μM TIC10 and their combinations. The data were normalized to the medium control. Data are presented as mean values \pm SD ($n = 3$). The levels of significance are shown as follows: $x: p < 0.05$; $y: p < 0.01$; $z: p < 0.001$.

4.2.3. The protein expression of death receptor 5 is increased after bortezomib treatment

TIC10 can induce apoptosis by binding the DR4 and DR5 receptors on the cell surface and by triggering the downstream signalling cascade (106, 107). Figure 20 A-B compares the data obtained from the experiments on the protein expression level of DR4 and DR5 on the surface of the A2058 melanoma cells. The expression of DR4 was impacted only due to the 13.5 μM TIC10 treatment (Figure 20 A). DR5 was affected by each of the investigated treatments, except for the 13.5 nM BOZ + 13.5 μM TIC10 co-treatment. However, when comparing the single treatments and co-treatments to each other, no significant difference was measured (Figure 20 B).

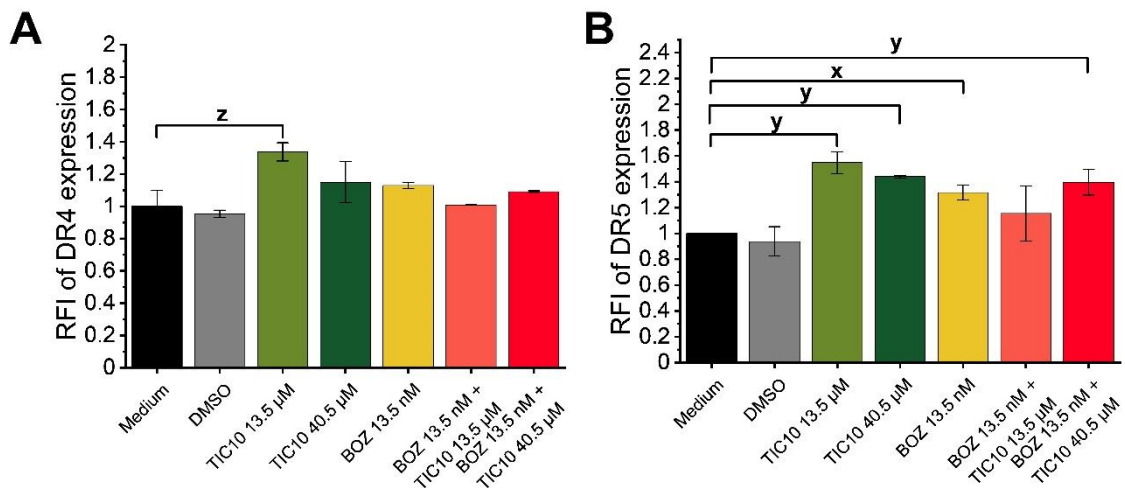


Figure 20 Influence on the death receptor 4 (DR4) and death receptor 5 (DR5) expression of melanoma cell line after 72h exposure. The ratio of the mean fluorescence intensity (RFI) of DR4 expression (A) and DR5 expression (B) is reported. The data were normalized to the medium control ($RFI = \text{treated cells MFI} / \text{control cells MFI}$; MFI: mean fluorescence intensity). Data are presented as mean values \pm SD ($n = 2$). The levels of significance are shown as follows: x: $p < 0.05$; y: $p < 0.01$; z: $p < 0.001$.

5. Discussion

In my thesis, two combinations of BOZ – one antagonistic with ALA and another synergistic with TIC10 – were presented. In both cases, we could use the Compusyn software to perform the analyses, as the CI value is capable to describe both types of interactions between drugs.

First, we found that BOZ showed an antitumor activity on the A2058 metastatic melanoma cell line ($IC_{50}=158$ nM) in 24h long experiments. This result is in line with the data found in the literature: that BOZ had cytotoxicity in vitro against a broad spectrum of solid tumors, including pancreatic, prostate, colorectal, head and neck, and ovarian cancers (100, 108, 109). However, it is clear that the reference – U266 cell line – was more sensitive than the A2058 cell line (IC_{50} : 2.17 nM vs. 158 nM, respectively). Contrary to the cell viability results, the IC_{50} values for proteasomal inhibition of BOZ slightly differed in the two cell lines (A2058— IC_{50} : 4.39 nM; U266— IC_{50} : 1.49 nM). In Phase I studies, BOZ proved to be safe and well-tolerated and the maximum tolerable dose (1.3 mg/m^2 - 1.75 mg/m^2) could be defined (110-112). Unfortunately, the patients enrolled in these Phase I clinical trials experienced multiple dose-limiting adverse events of BOZ, such as fatigue, anorexia, diarrhoea, thrombocytopenia, and neuropathy. However, Phase I studies had promising results regarding the antitumor effects. Phase II studies had rather controversial outcomes depending on the tumor type. Bortezomib had a lack of antitumor activity as a single agent curing malignant melanoma, however showed an antitumor effect in patients with advanced renal cell carcinoma (113, 114). In both studies, dose-limiting adverse events were identified, as a consequence either dose reduction was performed or the patient was removed from the study. These results call attention to the fact that either the dose-limiting side effects must be cured, or the dose must be reduced while combined with other anticancer agents.

In the first part of the thesis we screened how ALA and vit B1 could alter the effects of BOZ on a myeloma and melanoma cell line. These two neuroprotective agents were already proven to show efficacy in the treatment of diabetic neuropathy or anticancer drug-related neuropathy. Thus they may have a beneficial impact on the therapy of BIPN (115-118). These medicinal products are over-the-counter, and can be purchased without further medical supervision. Therefore the potential risks must be considered: while they may help to manage the symptoms of BIPN, they may also abolish the antitumor effect.

Unlike on U266 myeloma cells, we saw a drop in the anti-proliferative, as well as in the proteasome inhibitory effect of BOZ on A2058 melanoma cells, after the co-treatment with BOZ 20 ng/ml + ALA 100 µg/mL, as the number of the viable cells was increased compared to the BOZ-treated cells. Surprisingly, this alteration was not detectable in the apoptosis results. We hypothesized, that - as with many other anticancer drugs – BOZ could affect the malignant cells by disrupting the ROS homeostasis of the cells (119-121). Two tests were performed to analyze the oxidative status of the melanoma cells, a cell-based and a microscopic assay. The general ROS-promoting effect of BOZ was confirmed by the microscopic results, but when only the non-radical H₂O₂ level was measured post-BOZ treatment, no increase was seen in the A2058 cells. This controversy could be due to the high basal ROS content in the melanoma cells (122). It is worth mentioning that next to the oxygen containing reactive species, ROS, there are oxidative damage-causing molecules containing nitrogen (reactive nitrogen species) or sulfur atoms (reactive sulfur species) (123, 124). It is also possible that by detecting the oxidation status of the cells, we could detect other types of oxidation-causing radicals. Furthermore, BOZ could induce oxidative stress by elevating rather a wide range of oxidative radicals and not only H₂O₂ or other oxygen-containing radicals.

On the protein level, BOZ monotreatment caused cleavage of caspase-3 and upregulation of HO-1 expression in both cell lines, unlike claspin which was upregulated only in the melanoma cells. Both claspin and HO-1 are associated with the regulation of apoptosis, although different from caspases. Until caspases are responsible for the trigger of apoptosis, the programmed cell death, claspin and HO-1 may have protective roles, too (125-128). Claspin, as an adaptor protein has regulating role in the cell cycle and acts as a safeguard. When the genome integrity is disrupted, claspin takes part in deciding whether the cell cycle is arrested or continued (128, 129). The expression of HO-1 is induced by ROS; however, it may also contribute to carcinogenesis (130). It was shown, that BOZ can stimulate the expression of HO-1 in multiple myeloma cell lines (131).

We found that the level of 6 apoptosis-related proteins was downregulated in the BOZ 20 ng/mL + ALA 100 µg/mL treated melanoma cells in comparison to the BOZ 20 ng/mL treated cells (Hsp70, Hsp60, claspin, HO-1, cleaved caspase-3 and pro-caspase-3). Out of these 6 proteins, only 2 were downregulated following the combination treatment compared to the BOZ monotreatment in the myeloma cells (Hsp70, Hsp60). As no loss

of the antitumor effects of BOZ was detectable in the U266 cells, the variances in the amount of HO-1, claspin, and cleaved caspase-3 following BOZ or BOZ 20 ng/mL + ALA 100 µg/mL therapy may answer the different responses between the cell lines.

Taken together, we found that BOZ may have a tumor-specific pharmacodynamic effect. Our results also proved the in vitro efficacy of BOZ against solid tumors, such as metastatic melanoma cell lines. Unfortunately, evidence can be found in the literature, that during BOZ therapy, patients dealing with solid tumors can experience BIPN, a common adverse effect of BOZ therapy. Therefore, treatment of BIPN must be started while considering the possible interactions. We thought, that ALA could impair the effects of BOZ via its ROS scavenger effects, similarly to other ROS scavengers, e.g., NAC or glutathione-reduced ethyl ester, that are capable of reversing the BOZ-induced antiproliferative effects through the neutralization of ROS in Granta-519 and Jeko mantle-cell lymphoma cell lines (121). Unexpectedly, no impact of ALA was seen on the general oxidative status of the cells in our experiments. Among the reactive molecules, we know radicals with unpaired electrons (hydroxyl, superoxide, nitric oxide) and non-radical reactive species (H_2O_2 , ozone, nitrous acid) (75, 132). These radicals can be neutralized either by endogenous antioxidants (enzymatic, e.g., superoxide dismutase and catalase; non-enzymatic e.g., ALA or glutathione) or by exogenous antioxidants (e.g., vitamin E or vitamin C) (124, 133). The controversy in our results, that however, ALA is a known antioxidant, it was not able to suppress the general ROS-inducing effect of BOZ, may result from the antioxidant properties of ALA. Alpha-lipoic acid belongs to the non-enzymatic antioxidants, that can effectively regenerate other antioxidants, especially glutathione (117, 134). Glutathione is responsible for the decomposition of H_2O_2 in the cells (135). This may explain the drop in the H_2O_2 level in cells treated with BOZ+ALA compared to the monotreatment with BOZ. As a proteasome inhibitor, BOZ induces ER-stress and consequently the unfolded protein response (UPR), the accumulation of misfolded proteins within the ER due to the lack of the proteasomal degradation (136). The UPR can be considered as a homeostatic mechanism to buffer the ER stress associated ROS production and apoptosis (137). Alpha-lipoic acid may affect this UPR pathway induced by BOZ. This explanation seems to be supported by our results since we found that the level of pro-apoptotic proteins, e.g., claspin or HO-1 that are regulated via proteasomal degradation is increased after BOZ+ALA treatment compared to the

monotreatment with BOZ (138, 139). Taking together, ALA may not be a good candidate to treat BIPN due to the loss in the antitumor activity of BOZ when given in combination with ALA.

An option to overcome side effects is to utilize combinations where the dose of the antitumor drugs can be reduced (5, 8, 9). From 2017, our research group worked in collaboration (the National Competitiveness and Excellence Program, NVKP_16-1-2016-0036) with research groups led by Antal Csámpai from the Department of Organic Chemistry, Institute of Chemistry, Eötvös Lóránd University. This collaboration aimed to characterize more than 400 newly synthesized antitumor molecules. In this set of molecules, there was the TIC10 (also called ONC201) reference small molecule.

TIC10 belongs to the group of imipridones that were first tested as anti-seizure medications (140). In 2013, Allen and his co-workers identified it as a molecule with anticancer activity (87). The word TIC10 means “TRAIL-inducing compound 10”, which refers to its possible pharmacodynamics. Through the inactivation of the intracellular Akt/ERK pathway, FOXO3 gets dephosphorylated and this results in the upregulation of TRAIL (141). TRAIL is an agonist of the death receptors (DR4, DR5) presented on the cell surface. Its activation can promote apoptosis via the formation of a death-inducing signaling complex (DISC) and the downstream activation of caspases (142, 143). Related to the literature, the tumor cells in comparison to non-tumor cells overexpress these death receptors, so TIC10 might selectively target the tumor cells (144, 145). TIC10 was already investigated in combinations with the taxane paclitaxel and docetaxel in colon cancer and with lurbectedin against small cell lung cancer (87, 146). Thus, it seemed to be a potent candidate to investigate in combination with BOZ to reach synergism.

We found TIC10 to have antitumor activity against PANC1, COLO205, and EBC1 cells (1.7 ± 0.3 mM, 5.0 ± 2.9 μ M, and 7.0 ± 0.5 μ M, respectively), but not against A2058 cells. Based on the chemosensitizer activity of TIC10, we aimed to investigate whether (i) BOZ + TIC10 could have a synergistic antitumor effect against A2058 melanoma cells in order to find combinations where the dose of BOZ is minimal, while the antitumor effect remains due to the synergism between BOZ and TIC10. We found evidence in the literature that the expression of DR4 and DR5 is upregulated following a BOZ treatment in cancer cells, e.g., in HT-29 human colorectal adenocarcinoma cells and A549 human lung adenocarcinoma cells (147, 148). Next, we were curious whether the upregulation

of the death receptors can be detected in this synergistic relationship. Cell viability assays - after 72h long incubation - showed that, similarly to the results seen previously following 24h long incubations, BOZ inhibited the cell growth of U266 and A2058 cells (IC_{50} values: 1.45 nM and 23.07 nM, respectively). TIC10 was ineffective on the A2058 melanoma cells but inhibited the cell growth of the U266 cells (IC_{50} value: 0.97 μ M). Since synergism between BOZ and TIC10 was only detectable in this melanoma cell line, further experiments were not performed on the U266 cell line. The CompuSyn software defined three combinations (13.5 nM BOZ + 13.5 μ M TIC10; 13.5 nM BOZ + 40.5 μ M TIC10; 13.5 nM BOZ + 121 μ M TIC10), where the number of the viable cells after treatment with the BOZ+TIC10 combination is lower than in the matching monotreated cells and thus synergism was detected ($CI = 0.33, 0.25$ and 0.24 , respectively) (22). Despite the promising results, the 121 μ M TIC10-containing combination was excluded from the further analyses, as this solution contained 1.21 v/v% DMSO, which could already impact the cell viability according to the literature (105). It is important to note, that all of these combinations consist of 13.5 nM BOZ. That dose is under the IC_{50} value of BOZ (23.07 nM), determined on A2058 cells after a 72h long cell viability assay.

So far, cell viability was investigated in endpoint assays. The adherent characteristic of the A2058 melanoma cells allows the real-time investigation of cell viability in the xCELLigence SP system. This device can measure the changes in impedance over time and thus it can give information about cell viability in real-time (149). The results were a little unanticipated, as a subpopulation of the 13.5 nM BOZ-treated cells could proliferate, suggesting that acquired resistance to BOZ developed. This result is in line with results from the literature, where BOZ resistance was seen in vitro (e.g., non-small cell lung carcinoma) as well as in clinical (e.g., kappa light chain multiple myeloma) results (150-152). The growth of cells treated by the combination of BOZ+TIC10 remained to be inhibited. In addition, TIC10 treatment could enhance the antitumor effect of BOZ. The same tendency was observed in the apoptosis assay, more cells were Ax V/7AAD positive among the combination-treated cells, as in the monotreated ones. These experiments confirm previous results, that highlighted the greater responsiveness of resistant cells to chemotherapy (e.g., dexamethasone-resistant or bortezomib-resistant hematological cancer cell lines and 5-fluorouracil-resistant colorectal cancer stem/progenitor cells) following a TIC10 treatment (153-155).

Because TIC10 can upregulate the expression of TRAIL – the agonist ligand of death receptors – and thus it can initiate TRAIL-mediated apoptosis of tumor cells, we examined the DR4 and DR5 levels of the melanoma cells (87, 156, 157). The expression analyses showed the enhanced expression of DR5 in the BOZ and BOZ+TIC10 treated cells. This concurs well with earlier findings, where this up-regulation was also seen in HT-29 colorectal adenocarcinoma cells and in HCT116 colorectal carcinoma cells (147, 148, 158).

Taking ALA supplementation may be important for patients dealing with BIPN, but this treatment of this dose-limiting side effect of BOZ, can lead to a drop in the antitumor activity of BOZ during therapy. To solve this problem, combinatorial treatments can be used. In these combinations, the antitumor drugs can complement each other's effects, resulting in a synergistic activity. Thus, reduced doses can be utilized so the dose-limiting side effects can occur less often. Our results could prove this two-faced side of drug-drug interactions, on the one hand, they can be disadvantageous (ALA + BOZ), but on the other hand, they can be favourable (TIC10 + BOZ) (Figure 21).

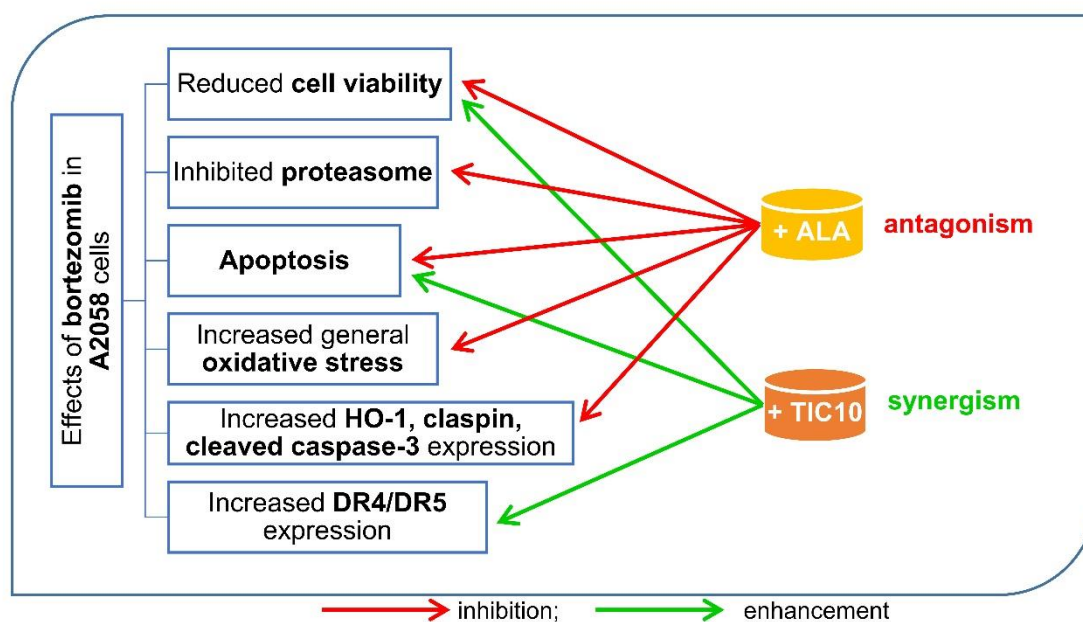


Figure 21 Summary of the effects of alpha-lipoic acid (ALA) or TIC10 on the effects of bortezomib (BOZ) in A2058 cells.

6. Conclusion

This thesis summarized the effects of BOZ+ALA and BOZ+TIC10 combinations in a melanoma cell line in vitro.

As a conclusion, our novel findings can demonstrate, that:

- Bortezomib has an antitumor effect against A2058 melanoma cells.
 - a. The neuroprotective ALA can abolish the BOZ-induced growth inhibition on A2058 cells and can diminish the proteasome inhibitory effect of BOZ.
 - b. In A2058 cells, the H₂O₂ level is stable following a BOZ treatment, however, the general oxidative status of the cells is elevated.
 - c. Changes in the level of HO-1, claspin, and cleaved caspase-3 protein can explain the antagonism between BOZ and ALA.
- TIC10 does not affect the viability of the A2058 cells.
- A2058 cells can lose their sensitivity to BOZ in a long term manner (after 48-72h).
- BOZ + TIC10, when given together, can synergize.
 - a. The dose of BOZ in the synergistic combinations is almost half of the IC₅₀ dose on A2058 cells (13.5 nM vs. 23.07 nM, respectively).
 - b. BOZ and BOZ + TIC10 combination can upregulate the expression of DR5, which is a receptor of TRAIL, a potential target of TIC10.
 - c. In combinations, the doses of the different drugs can be lowered, therefore dose-limiting side effects may be prevented.

7. Summary

Melanoma is a leading cause of death worldwide. Unfortunately, it remains hardly curable, thus new therapeutic approaches are always needed. In our project, we investigated whether (bortezomib) BOZ, a proteasome inhibitor may have antitumor effects against a metastatic melanoma cell line. We found that – in short-term experiments – BOZ reduced the the number of viable cells by inducing apoptosis .

In clinical practice, most of the BOZ-treated patients with hematologic or solid malignancies experience bortezomib-induced peripheral neuropathy (BIPN), one of the dose-limiting side effects. The quality of life of the patients must be maintained during chemotherapy, but the prevention and treatment of BIPN is a big challenge. Alpha-lipoic acid (ALA), a neuroprotective agent, proved its effectiveness many times in different types of neuropathy. However, we found that it may also reduce the proteasome inhibitory effect of BOZ, which results in the loss of its antiproliferative effects. Differently influenced HO-1, claspin, caspase-3 and H₂O₂ level may stand in the background of the antagonism between BOZ and ALA. So utilization of ALA to treat BIPN in patients dealing with melanoma may be problematic.

The next possibility is to reduce the dose of BOZ, but to maintain its effectiveness, thus it has to be combined with another antitumour agent. After analyzing the pharmacodynamics of BOZ, we found that the TRAIL-inducing compound 10 (TIC10), a TNF-Related Apoptosis Inducing Ligand (TRAIL) inducer, can synergize with BOZ. The death receptor 5 (DR5) expression is upregulated in the BOZ-treated cells. Based on the literature, the possible explanation for this synergism that the simultaneously utilized TIC10 treatment may lead to TRAIL expression, which can then bind and activate the DR5 which is upregulated due to the BOZ therapy.

Our results on A2058 melanoma cells suggest that BOZ could be antagonized by ALA, however, it synergizes with TIC10, so the development of dose-limiting side effects, e.g., BIPN could be prevented by combinatorial treatments.

8. References

1. Frei E, Karon M, Levin RH, Freireich EJ, Taylor RJ, Hananian J, Selawry O, Holland JF, Hoogstraten B, Wolman IJ, Abir E, Sawitsky A, Lee S, Mills SD, Burgert EO, Jr., Spurr CL, Patterson RB, Ebaugh FG, James GW, 3rd, Moon JH. The effectiveness of combinations of antileukemic agents in inducing and maintaining remission in children with acute leukemia. *Blood*. 1965;26(5):642-656.
2. Al-Lazikani B, Banerji U, Workman P. Combinatorial drug therapy for cancer in the post-genomic era. *Nat Biotechnol*. 2012;30(7):679-692.
3. Shyr ZA, Cheng YS, Lo DC, Zheng W. Drug combination therapy for emerging viral diseases. *Drug Discov Today*. 2021;26(10):2367-2376.
4. Clemmensen C, Finan B, Müller TD, DiMarchi RD, Tschöp MH, Hofmann SM. Emerging hormonal-based combination pharmacotherapies for the treatment of metabolic diseases. *Nat Rev Endocrinol*. 2019;15(2):90-104.
5. Bayat Mokhtari R, Homayouni TS, Baluch N, Morgatskaya E, Kumar S, Das B, Yeger H. Combination therapy in combating cancer. *Oncotarget*. 2017;8(23):38022-38043.
6. Mukherjee B, Howard L. Combination therapy in pulmonary arterial hypertension: do we have the right strategy? *Expert Rev Respir Med*. 2011;5(2):191-205.
7. Al-Zakwani I, Zubaid M, Panduranga P, Rashed W, Sulaiman K, Almahmeed W, Al-Motarreb A, Al Suwaidi J, Amin H. Medication use pattern and predictors of optimal therapy at discharge in 8176 patients with acute coronary syndrome from 6 Middle Eastern countries: data from the gulf registry of acute coronary events. *Angiology*. 2011;62(6):447-454.
8. Bukowska B, Gajek A, Marczak A. Two drugs are better than one. A short history of combined therapy of ovarian cancer. *Contemp Oncol (Pozn)*. 2015;19(5):350-353.
9. Ascierto PA, Marincola FM. Combination therapy: the next opportunity and challenge of medicine. *J Transl Med*. 2011;9:115.
10. Wang B, Warden AR, Ding X. The optimization of combinatorial drug therapies: Strategies and laboratorial platforms. *Drug Discov Today*. 2021;26(11):2646-2659.
11. Ismail M, Khan S, Khan F, Noor S, Sajid H, Yar S, Rasheed I. Prevalence and significance of potential drug-drug interactions among cancer patients receiving chemotherapy. *BMC Cancer*. 2020;20(1):335.

12. Tolcher AW, Mayer LD. Improving combination cancer therapy: the CombiPlex(®) development platform. *Future Oncol.* 2018;14(13):1317-1332.
13. Delgado A, Guddati AK. Clinical endpoints in oncology - a primer. *Am J Cancer Res.* 2021;11(4):1121-1131.
14. Rationalizing combination therapies. *Nature Medicine.* 2017;23(10):1113-1113.
15. Chou TC. Theoretical basis, experimental design, and computerized simulation of synergism and antagonism in drug combination studies. *Pharmacol Rev.* 2006;58(3):621-681.
16. García-Fuente A, Vázquez F, Viéitez JM, García Alonso FJ, Martín JI, Ferrer J. CISNE: An accurate description of dose-effect and synergism in combination therapies. *Sci Rep.* 2018;8(1):4964.
17. Roell KR, Reif DM, Motsinger-Reif AA. An Introduction to Terminology and Methodology of Chemical Synergy-Perspectives from Across Disciplines. *Front Pharmacol.* 2017;8:158.
18. 2023 [Available from: https://www.researchgate.net/publication/16813250_Quantitative_Analysis_of_Dose-Effect_Relationships_The_Combined_Effects_of_Multiple_Drugs_or_Enzyme_Inhibitors/citations.
19. Chou TC. Drug combination studies and their synergy quantification using the Chou-Talalay method. *Cancer Res.* 2010;70(2):440-446.
20. Ma J, Motsinger-Reif A. Current Methods for Quantifying Drug Synergism. *Proteom Bioinform.* 2019;1(2):43-48.
21. ComboSyn I. januar, 2021 [Available from: <https://www.combosyn.com/>].
22. Chou TC. Preclinical versus clinical drug combination studies. *Leuk Lymphoma.* 2008;49(11):2059-2080.
23. Wagstaff W, Mwamba RN, Grullon K, Armstrong M, Zhao P, Hendren-Santiago B, Qin KH, Li AJ, Hu DA, Youssef A, Reid RR, Luu HH, Shen L, He TC, Haydon RC. Melanoma: Molecular genetics, metastasis, targeted therapies, immunotherapies, and therapeutic resistance. *Genes Dis.* 2022;9(6):1608-1623.
24. Yang K, Oak ASW, Slominski RM, Brożyna AA, Slominski AT. Current Molecular Markers of Melanoma and Treatment Targets. *International journal of molecular sciences.* 2020;21(10):3535.

25. Leonardi GC, Falzone L, Salemi R, Zanghì A, Spandidos DA, McCubrey JA, Candido S, Libra M. Cutaneous melanoma: From pathogenesis to therapy (Review). *Int J Oncol*. 2018;52(4):1071-1080.
26. Gandini S, Sera F, Cattaruzza MS, Pasquini P, Picconi O, Boyle P, Melchi CF. Meta-analysis of risk factors for cutaneous melanoma: II. Sun exposure. *Eur J Cancer*. 2005;41(1):45-60.
27. Rastogi RP, Richa, Kumar A, Tyagi MB, Sinha RP. Molecular mechanisms of ultraviolet radiation-induced DNA damage and repair. *J Nucleic Acids*. 2010;2010:592980.
28. Sample A, He YY. Mechanisms and prevention of UV-induced melanoma. *Photodermatol Photoimmunol Photomed*. 2018;34(1):13-24.
29. Davis LE, Shalin SC, Tackett AJ. Current state of melanoma diagnosis and treatment. *Cancer Biol Ther*. 2019;20(11):1366-1379.
30. Rossi M, Pellegrini C, Cardelli L, Ciciarelli V, Di Nardo L, Fargnoli MC. Familial Melanoma: Diagnostic and Management Implications. *Dermatol Pract Concept*. 2019;9(1):10-16.
31. Bastian BC. The molecular pathology of melanoma: an integrated taxonomy of melanocytic neoplasia. *Annu Rev Pathol*. 2014;9:239-271.
32. Curtin JA, Fridlyand J, Kageshita T, Patel HN, Busam KJ, Kutzner H, Cho KH, Aiba S, Bröcker EB, LeBoit PE, Pinkel D, Bastian BC. Distinct sets of genetic alterations in melanoma. *N Engl J Med*. 2005;353(20):2135-2147.
33. Damsky WE, Rosenbaum LE, Bosenberg M. Decoding melanoma metastasis. *Cancers (Basel)*. 2010;3(1):126-163.
34. Eisen T, Ahmad T, Flaherty KT, Gore M, Kaye S, Marais R, Gibbens I, Hackett S, James M, Schuchter LM, Nathanson KL, Xia C, Simantov R, Schwartz B, Poulin-Costello M, O'Dwyer PJ, Ratain MJ. Sorafenib in advanced melanoma: a Phase II randomised discontinuation trial analysis. *Br J Cancer*. 2006;95(5):581-586.
35. Goldberg AL. Functions of the proteasome: from protein degradation and immune surveillance to cancer therapy. *Biochem Soc Trans*. 2007;35(Pt 1):12-17.
36. Krämer L, Groh C, Herrmann JM. The proteasome: friend and foe of mitochondrial biogenesis. *FEBS Lett*. 2021;595(8):1223-1238.

37. Adams J. The proteasome: structure, function, and role in the cell. *Cancer Treatment Reviews*. 2003;29:3-9.
38. Jäger S, Groll M, Huber R, Wolf DH, Heinemeyer W. Proteasome beta-type subunits: unequal roles of propeptides in core particle maturation and a hierarchy of active site function. *J Mol Biol*. 1999;291(4):997-1013.
39. Kubiczikova L, Pour L, Sedlarikova L, Hajek R, Sevcikova S. Proteasome inhibitors - molecular basis and current perspectives in multiple myeloma. *J Cell Mol Med*. 2014;18(6):947-961.
40. Almond JB, Cohen GM. The proteasome: a novel target for cancer chemotherapy. *Leukemia*. 2002;16(4):433-443.
41. Navon A, Ciechanover A. The 26 S proteasome: from basic mechanisms to drug targeting. *J Biol Chem*. 2009;284(49):33713-33718.
42. Glickman MH, Ciechanover A. The ubiquitin-proteasome proteolytic pathway: destruction for the sake of construction. *Physiol Rev*. 2002;82(2):373-428.
43. Rastogi N, Mishra DP. Therapeutic targeting of cancer cell cycle using proteasome inhibitors. *Cell Div*. 2012;7(1):26.
44. Rastogi N, Duggal S, Singh SK, Porwal K, Srivastava VK, Maurya R, Bhatt ML, Mishra DP. Proteasome inhibition mediates p53 reactivation and anti-cancer activity of 6-gingerol in cervical cancer cells. *Oncotarget*. 2015;6(41):43310-43325.
45. Wu WK, Cho CH, Lee CW, Wu K, Fan D, Yu J, Sung JJ. Proteasome inhibition: a new therapeutic strategy to cancer treatment. *Cancer Lett*. 2010;293(1):15-22.
46. Shahshahan MA, Beckley MN, Jazirehi AR. Potential usage of proteasome inhibitor bortezomib (Velcade, PS-341) in the treatment of metastatic melanoma: basic and clinical aspects. *Am J Cancer Res*. 2011;1(7):913-924.
47. Landis-Piowar KR, Huo C, Chen D, Milacic V, Shi G, Chan TH, Dou QP. A novel prodrug of the green tea polyphenol (-)-epigallocatechin-3-gallate as a potential anticancer agent. *Cancer Res*. 2007;67(9):4303-4310.
48. O'Sullivan-Coyne G, O'Sullivan GC, O'Donovan TR, Piwocka K, McKenna SL. Curcumin induces apoptosis-independent death in oesophageal cancer cells. *Br J Cancer*. 2009;101(9):1585-1595.

49. Richardson PG, Hideshima T, Anderson KC. Bortezomib (PS-341): a novel, first-in-class proteasome inhibitor for the treatment of multiple myeloma and other cancers. *Cancer Control*. 2003;10(5):361-369.
50. Adams J, Palombella VJ, Sausville EA, Johnson J, Destree A, Lazarus DD, Maas J, Pien CS, Prakash S, Elliott PJ. Proteasome inhibitors: a novel class of potent and effective antitumor agents. *Cancer Res*. 1999;59(11):2615-2622.
51. Adams J, Kauffman M. Development of the proteasome inhibitor Velcade (Bortezomib). *Cancer Invest*. 2004;22(2):304-311.
52. Groll M, Huber R, Moroder L. The persisting challenge of selective and specific proteasome inhibition. *J Pept Sci*. 2009;15(2):58-66.
53. Jayaweera SPE, Wanigasinghe Kanakanamge SP, Rajalingam D, Silva GN. Carfilzomib: A Promising Proteasome Inhibitor for the Treatment of Relapsed and Refractory Multiple Myeloma. *Front Oncol*. 2021;11:740796.
54. Kane RC, Bross PF, Farrell AT, Pazdur R. Velcade®: U.S. FDA Approval for the Treatment of Multiple Myeloma Progressing on Prior Therapy. *The Oncologist*. 2003;8(6):508-513.
55. Bladé J, Cibeira MT, Rosiñol L. Bortezomib: A valuable new antineoplastic strategy in multiple myeloma. *Acta Oncologica*. 2005;44(5):440-448.
56. Raedler L. Velcade (Bortezomib) Receives 2 New FDA Indications: For Retreatment of Patients with Multiple Myeloma and for First-Line Treatment of Patients with Mantle-Cell Lymphoma. *Am Health Drug Benefits*. 2015;8(Spec Feature):135-140.
57. Griger Z, Tóth BI, Baráth S, Gyetvai Á, Kovács I, Tarr T, Bíró T, Zeher M, Sipka S. Different effects of bortezomib on the expressions of various protein kinase C isoenzymes in T cells of patients with systemic lupus erythematosus and in Jurkat cells. *Scand J Immunol*. 2012;75(2):243-248.
58. Pasquale R, Giannotta JA, Barcellini W, Fattizzo B. Bortezomib in autoimmune hemolytic anemia and beyond. *Ther Adv Hematol*. 2021;12:20406207211046428.
59. Gomez AM, Willcox N, Molenaar PC, Buurman W, Martinez-Martinez P, De Baets MH, Losen M. Targeting plasma cells with proteasome inhibitors: possible roles in treating myasthenia gravis? *Ann N Y Acad Sci*. 2012;1274:48-59.
60. Markowitz J, Luedke EA, Grignol VP, Hade EM, Paul BK, Mundy-Bosse BL, Brooks TR, Dao TV, Kondalasula SV, Lesinski GB, Olencki T, Kendra KL, Carson WE,

- 3rd. A phase I trial of bortezomib and interferon- α -2b in metastatic melanoma. *J Immunother*. 2014;37(1):55-62.
61. Field-Smith A, Morgan GJ, Davies FE. Bortezomib (Velcade[®] trade mark) in the Treatment of Multiple Myeloma. *Ther Clin Risk Manag*. 2006;2(3):271-279.
62. Xia Y, Shen S, Verma IM. NF- κ B, an active player in human cancers. *Cancer Immunol Res*. 2014;2(9):823-830.
63. Qin JZ, Ziffra J, Stennett L, Bodner B, Bonish BK, Chaturvedi V, Bennett F, Pollock PM, Trent JM, Hendrix MJ, Rizzo P, Miele L, Nickoloff BJ. Proteasome inhibitors trigger NOXA-mediated apoptosis in melanoma and myeloma cells. *Cancer Res*. 2005;65(14):6282-6293.
64. Chen D, Frezza M, Schmitt S, Kanwar J, Dou QP. Bortezomib as the first proteasome inhibitor anticancer drug: current status and future perspectives. *Curr Cancer Drug Targets*. 2011;11(3):239-253.
65. Fribley A, Zeng Q, Wang CY. Proteasome inhibitor PS-341 induces apoptosis through induction of endoplasmic reticulum stress-reactive oxygen species in head and neck squamous cell carcinoma cells. *Mol Cell Biol*. 2004;24(22):9695-9704.
66. Jagannath S, Durie BG, Wolf J, Camacho E, Irwin D, Lutzky J, McKinley M, Gabayan E, Mazumder A, Schenkein D, Crowley J. Bortezomib therapy alone and in combination with dexamethasone for previously untreated symptomatic multiple myeloma. *Br J Haematol*. 2005;129(6):776-783.
67. Robak T, Huang H, Jin J, Zhu J, Liu T, Samoilova O, Pylypenko H, Verhoef G, Siritanaratkul N, Osmanov E, Alexeeva J, Pereira J, Drach J, Mayer J, Hong X, Okamoto R, Pei L, Rooney B, van de Velde H, Cavalli F. Bortezomib-based therapy for newly diagnosed mantle-cell lymphoma. *N Engl J Med*. 2015;372(10):944-953.
68. Staff NP, Windebank AJ. Peripheral neuropathy due to vitamin deficiency, toxins, and medications. *Continuum (Minneapolis, Minn)*. 2014;20(5 Peripheral Nervous System Disorders):1293-1306.
69. Cavaletti G, Jakubowiak AJ. Peripheral neuropathy during bortezomib treatment of multiple myeloma: a review of recent studies. *Leuk Lymphoma*. 2010;51(7):1178-1187.
70. Carozzi VA, Canta A, Chiorazzi A. Chemotherapy-induced peripheral neuropathy: What do we know about mechanisms? *Neurosci Lett*. 2015;596:90-107.

71. Han Y, Smith MT. Pathobiology of cancer chemotherapy-induced peripheral neuropathy (CIPN). *Front Pharmacol*. 2013;4:156.
72. Yamamoto S, Egashira N. Pathological Mechanisms of Bortezomib-Induced Peripheral Neuropathy. *International journal of molecular sciences*. 2021;22(2).
73. Mu SD, Ai LS, Qin Y, Hu Y. Subcutaneous versus Intravenous Bortezomib Administration for Multiple Myeloma Patients: a Meta-analysis. *Curr Med Sci*. 2018;38(1):43-50.
74. Richardson PG, Briemberg H, Jagannath S, Wen PY, Barlogie B, Berenson J, Singhal S, Siegel DS, Irwin D, Schuster M, Srkalovic G, Alexanian R, Rajkumar SV, Limentani S, Alsina M, Orlowski RZ, Najarian K, Esseltine D, Anderson KC, Amato AA. Frequency, characteristics, and reversibility of peripheral neuropathy during treatment of advanced multiple myeloma with bortezomib. *J Clin Oncol*. 2006;24(19):3113-3120.
75. Ray PD, Huang BW, Tsuji Y. Reactive oxygen species (ROS) homeostasis and redox regulation in cellular signaling. *Cell Signal*. 2012;24(5):981-990.
76. Mohty B, El-Cheikh J, Yakoub-Agha I, Moreau P, Harousseau JL, Mohty M. Peripheral neuropathy and new treatments for multiple myeloma: background and practical recommendations. *Haematologica*. 2010;95(2):311-319.
77. Yan W, Wu Z, Zhang Y, Hong D, Dong X, Liu L, Rao Y, Huang L, Zhang X, Wu J. The molecular and cellular insight into the toxicology of bortezomib-induced peripheral neuropathy. *Biomed Pharmacother*. 2021;142:112068.
78. Nakano A, Abe M, Oda A, Amou H, Hiasa M, Nakamura S, Miki H, Harada T, Fujii S, Kagawa K, Takeuchi K, Watanabe T, Ozaki S, Matsumoto T. Delayed treatment with vitamin C and N-acetyl-L-cysteine protects Schwann cells without compromising the anti-myeloma activity of bortezomib. *Int J Hematol*. 2011;93(6):727-735.
79. Ang CD, Alviar MJ, Dans AL, Bautista-Velez GG, Villaruz-Sulit MV, Tan JJ, Co HU, Bautista MR, Roxas AA. Vitamin B for treating peripheral neuropathy. *Cochrane Database Syst Rev*. 2008(3):Cd004573.
80. Catley L, Anderson KC. Velcade and vitamin C: too much of a good thing? *Clin Cancer Res*. 2006;12(1):3-4.
81. Flühmann B, Ntai I, Borchard G, Simoens S, Mühlebach S. Nanomedicines: The magic bullets reaching their target? *Eur J Pharm Sci*. 2019;128:73-80.

82. Atreja A, Bellam N, Levy SR. Strategies to enhance patient adherence: making it simple. *MedGenMed*. 2005;7(1):4.
83. Chhabra M. Chapter 6 - Biological therapeutic modalities. In: Hasija Y, editor. *Translational Biotechnology*: Academic Press; 2021. p. 137-164.
84. Ngo HX, Garneau-Tsodikova S. What are the drugs of the future? *Medchemcomm*. 2018;9(5):757-758.
85. Sylvester K, Rocchio M, Beik N, Fanikos J. Biosimilars: An Emerging Category of Biologic Drugs for Emergency Medicine Practitioners. *Current Emergency and Hospital Medicine Reports*. 2013;1(4):226-235.
86. Allen JE, Kline CL, Prabhu VV, Wagner J, Ishizawa J, Madhukar N, Lev A, Baumeister M, Zhou L, Lulla A, Stogniew M, Schalop L, Benes C, Kaufman HL, Pottorf RS, Nallaganchu BR, Olson GL, Al-Mulla F, Duvic M, Wu GS, Dicker DT, Talekar MK, Lim B, Elemento O, Oster W, Bertino J, Flaherty K, Wang ML, Borthakur G, Andreeff M, Stein M, El-Deiry WS. Discovery and clinical introduction of first-in-class imipridone ONC201. *Oncotarget*. 2016;7(45):74380-74392.
87. Allen JE, Krigsfeld G, Mayes PA, Patel L, Dicker DT, Patel AS, Dolloff NG, Messaris E, Scata KA, Wang W, Zhou JY, Wu GS, El-Deiry WS. Dual inactivation of Akt and ERK by TIC10 signals Foxo3a nuclear translocation, TRAIL gene induction, and potent antitumor effects. *Sci Transl Med*. 2013;5(171):171ra117.
88. Kline CL, Van den Heuvel AP, Allen JE, Prabhu VV, Dicker DT, El-Deiry WS. ONC201 kills solid tumor cells by triggering an integrated stress response dependent on ATF4 activation by specific eIF2 α kinases. *Sci Signal*. 2016;9(415):ra18.
89. Endo Greer Y, Lipkowitz S. ONC201: Stressing tumors to death. *Sci Signal*. 2016;9(415):fs1.
90. Wagner J, Kline CL, Zhou L, Campbell KS, MacFarlane AW, Olszanski AJ, Cai KQ, Hensley HH, Ross EA, Ralff MD, Zloza A, Chesson CB, Newman JH, Kaufman H, Bertino J, Stein M, El-Deiry WS. Dose intensification of TRAIL-inducing ONC201 inhibits metastasis and promotes intratumoral NK cell recruitment. *J Clin Invest*. 2018;128(6):2325-2338.
91. Yuan X, Gajan A, Chu Q, Xiong H, Wu K, Wu GS. Developing TRAIL/TRAIL death receptor-based cancer therapies. *Cancer Metastasis Rev*. 2018;37(4):733-748.

92. Arrillaga-Romany I, Chi AS, Allen JE, Oster W, Wen PY, Batchelor TT. A phase 2 study of the first imipridone ONC201, a selective DRD2 antagonist for oncology, administered every three weeks in recurrent glioblastoma. *Oncotarget*. 2017;8(45):79298-79304.
93. Stein MN, Bertino JR, Kaufman HL, Mayer T, Moss R, Silk A, Chan N, Malhotra J, Rodriguez L, Aisner J, Aiken RD, Haffty BG, DiPaola RS, Saunders T, Zloza A, Damare S, Beckett Y, Yu B, Najmi S, Gabel C, Dickerson S, Zheng L, El-Deiry WS, Allen JE, Stogniew M, Oster W, Mehnert JM. First-in-Human Clinical Trial of Oral ONC201 in Patients with Refractory Solid Tumors. *Clin Cancer Res*. 2017;23(15):4163-4169.
94. Nii T, Prabhu VV, Ruvolo V, Madhukar N, Zhao R, Mu H, Heese L, Nishida Y, Kojima K, Garnett MJ, McDermott U, Benes CH, Charter N, Deacon S, Elemento O, Allen JE, Oster W, Stogniew M, Ishizawa J, Andreeff M. Imipridone ONC212 activates orphan G protein-coupled receptor GPR132 and integrated stress response in acute myeloid leukemia. *Leukemia*. 2019;33(12):2805-2816.
95. Reece DE, Sullivan D, Lonial S, Mohrbacher AF, Chatta G, Shustik C, Burris H, 3rd, Venkatakrishnan K, Neuwirth R, Riordan WJ, Karol M, von Moltke LL, Acharya M, Zannikos P, Keith Stewart A. Pharmacokinetic and pharmacodynamic study of two doses of bortezomib in patients with relapsed multiple myeloma. *Cancer Chemother Pharmacol*. 2011;67(1):57-67.
96. Shay KP, Moreau RF, Smith EJ, Smith AR, Hagen TM. Alpha-lipoic acid as a dietary supplement: molecular mechanisms and therapeutic potential. *Biochim Biophys Acta*. 2009;1790(10):1149-1160.
97. Smithline HA, Donnino M, Greenblatt DJ. Pharmacokinetics of high-dose oral thiamine hydrochloride in healthy subjects. *BMC Clin Pharmacol*. 2012;12:4.
98. Tenório M, Graciliano NG, Moura FA, Oliveira ACM, Goulart MOF. N-Acetylcysteine (NAC): Impacts on Human Health. *Antioxidants (Basel)*. 2021;10(6).
99. Zhitkovich A. N-Acetylcysteine: Antioxidant, Aldehyde Scavenger, and More. *Chemical Research in Toxicology*. 2019;32(7):1318-1319.
100. Russo A, Fratto ME, Bazan V, Schiró V, Agnese V, Cicero G, Vincenzi B, Tonini G, Santini D. Targeting apoptosis in solid tumors: the role of bortezomib from preclinical to clinical evidence. *Expert Opin Ther Targets*. 2007;11(12):1571-1586.

101. Caravita T, de Fabritiis P, Palumbo A, Amadori S, Boccadoro M. Bortezomib: efficacy comparisons in solid tumors and hematologic malignancies. *Nat Clin Pract Oncol.* 2006;3(7):374-387.
102. Shi C, Gu Z, Xu S, Ju H, Wu Y, Han Y, Li J, Li C, Wu J, Wang L, Li J, Zhou G, Ye W, Ren G, Zhang Z, Zhou R. Candidate therapeutic agents in a newly established triple wild-type mucosal melanoma cell line. *Cancer Commun (Lond).* 2022;42(7):627-647.
103. Teichert J, Hermann R, Ruus P, Preiss R. Plasma kinetics, metabolism, and urinary excretion of alpha-lipoic acid following oral administration in healthy volunteers. *J Clin Pharmacol.* 2003;43(11):1257-1267.
104. Bárány P, Oláh RS, Kovács I, Czuczi T, Szabó CL, Takács A, Lajkó E, Láng O, Kőhidai L, Schlosser G, Bősze S, Mező G, Hudecz F, Csámpai A. Ferrocene-Containing Impiridone (ONC201) Hybrids: Synthesis, DFT Modelling, In Vitro Evaluation, and Structure–Activity Relationships. *Molecules.* 2018;23(9).
105. Chen X, Thibeault S. Effect of DMSO concentration, cell density and needle gauge on the viability of cryopreserved cells in three dimensional hyaluronan hydrogel. *Annu Int Conf IEEE Eng Med Biol Soc.* 2013;2013:6228-6231.
106. Wang G, Wang X, Yu H, Wei S, Williams N, Holmes DL, Halfmann R, Naidoo J, Wang L, Li L, Chen S, Harran P, Lei X, Wang X. Small-molecule activation of the TRAIL receptor DR5 in human cancer cells. *Nat Chem Biol.* 2013;9(2):84-89.
107. Artykov AA, Yagolovich AV, Dolgikh DA, Kirpichnikov MP, Trushina DB, Gasparian ME. Death Receptors DR4 and DR5 Undergo Spontaneous and Ligand-Mediated Endocytosis and Recycling Regardless of the Sensitivity of Cancer Cells to TRAIL. *Front Cell Dev Biol.* 2021;9:733688.
108. Frankel A, Man S, Elliott P, Adams J, Kerbel RS. Lack of multicellular drug resistance observed in human ovarian and prostate carcinoma treated with the proteasome inhibitor PS-341. *Clin Cancer Res.* 2000;6(9):3719-3728.
109. Mujtaba T, Dou QP. Advances in the understanding of mechanisms and therapeutic use of bortezomib. *Discov Med.* 2011;12(67):471-480.
110. Su Y, Amiri KI, Horton LW, Yu Y, Ayers GD, Koehler E, Kelley MC, Puzanov I, Richmond A, Sosman JA. A phase I trial of bortezomib with temozolomide in patients

with advanced melanoma: toxicities, antitumor effects, and modulation of therapeutic targets. *Clin Cancer Res.* 2010;16(1):348-357.

111. Aghajanian C, Soignet S, Dizon DS, Pien CS, Adams J, Elliott PJ, Sabbatini P, Miller V, Hensley ML, Pezzulli S, Canales C, Daud A, Spriggs DR. A phase I trial of the novel proteasome inhibitor PS341 in advanced solid tumor malignancies. *Clin Cancer Res.* 2002;8(8):2505-2511.

112. Hamilton AL, Eder JP, Pavlick AC, Clark JW, Liebes L, Garcia-Carbonero R, Chachoua A, Ryan DP, Soma V, Farrell K, Kinchla N, Boyden J, Yee H, Zeleniuch-Jacquotte A, Wright J, Elliott P, Adams J, Muggia FM. Proteasome inhibition with bortezomib (PS-341): a phase I study with pharmacodynamic end points using a day 1 and day 4 schedule in a 14-day cycle. *J Clin Oncol.* 2005;23(25):6107-6116.

113. Kondagunta GV, Drucker B, Schwartz L, Bacik J, Marion S, Russo P, Mazumdar M, Motzer RJ. Phase II trial of bortezomib for patients with advanced renal cell carcinoma. *J Clin Oncol.* 2004;22(18):3720-3725.

114. Markovic SN, Geyer SM, Dawkins F, Sharfman W, Albertini M, Maples W, Fracasso PM, Fitch T, Lorusso P, Adjei AA, Erlichman C. A phase II study of bortezomib in the treatment of metastatic malignant melanoma. *Cancer.* 2005;103(12):2584-2589.

115. Luong KV, Nguyen LT. The impact of thiamine treatment in the diabetes mellitus. *J Clin Med Res.* 2012;4(3):153-160.

116. Gedlicka C, Kornek GV, Schmid K, Scheithauer W. Amelioration of docetaxel/cisplatin induced polyneuropathy by alpha-lipoic acid. *Ann Oncol.* 2003;14(2):339-340.

117. Golbidi S, Badran M, Laher I. Diabetes and alpha lipoic Acid. *Front Pharmacol.* 2011;2:69.

118. Maschio M, Zarabla A, Maialetti A, Marchesi F, Giannarelli D, Gumenyuk S, Pisani F, Renzi D, Galiè E, Mengarelli A. Prevention of Bortezomib-Related Peripheral Neuropathy With Docosahexaenoic Acid and α -Lipoic Acid in Patients With Multiple Myeloma: Preliminary Data. *Integr Cancer Ther.* 2018;17(4):1115-1124.

119. Kim SJ, Kim HS, Seo YR. Understanding of ROS-Inducing Strategy in Anticancer Therapy. *Oxid Med Cell Longev.* 2019;2019:5381692.

120. Moloney JN, Cotter TG. ROS signalling in the biology of cancer. *Semin Cell Dev Biol.* 2018;80:50-64.

121. Pérez-Galán P, Roué G, Villamor N, Montserrat E, Campo E, Colomer D. The proteasome inhibitor bortezomib induces apoptosis in mantle-cell lymphoma through generation of ROS and Noxa activation independent of p53 status. *Blood*. 2006;107(1):257-264.
122. Zhang X, Li H, Liu C, Yuan X. Role of ROS-mediated autophagy in melanoma (Review). *Mol Med Rep*. 2022;26(4).
123. Di Meo S, Reed TT, Venditti P, Victor VM. Role of ROS and RNS Sources in Physiological and Pathological Conditions. *Oxid Med Cell Longev*. 2016;2016:1245049.
124. Martemucci G, Costagliola C, Mariano M, D'andrea L, Napolitano P, D'Alessandro AG. Free Radical Properties, Source and Targets, Antioxidant Consumption and Health. *Oxygen*. 2022;2(2):48-78.
125. Porter AG, Jänicke RU. Emerging roles of caspase-3 in apoptosis. *Cell Death Differ*. 1999;6(2):99-104.
126. Iskandarani A, Bhat AA, Siveen KS, Prabhu KS, Kuttikrishnan S, Khan MA, Krishnankutty R, Kulinski M, Nasr RR, Mohammad RM, Uddin S. Bortezomib-mediated downregulation of S-phase kinase protein-2 (SKP2) causes apoptotic cell death in chronic myelogenous leukemia cells. *J Transl Med*. 2016;14:69.
127. Liu ZM, Chen GG, Ng EK, Leung WK, Sung JJ, Chung SC. Upregulation of heme oxygenase-1 and p21 confers resistance to apoptosis in human gastric cancer cells. *Oncogene*. 2004;23(2):503-513.
128. Azenha D, Lopes MC, Martins TC. Claspin functions in cell homeostasis-A link to cancer? *DNA Repair (Amst)*. 2017;59:27-33.
129. Hsiao H-W, Yang C-C, Masai H. Roles of Claspin in regulation of DNA replication, replication stress responses and oncogenesis in human cells. *Genome Instability & Disease*. 2021;2(5):263-280.
130. Bahmani P, Hassanshahi G, Halabian R, Roushandeh AM, Jahanian-Najafabadi A, Roudkenar MH. The expression of heme oxygenase-1 in human-derived cancer cell lines. *Iran J Med Sci*. 2011;36(4):260-265.
131. Barrera LN, Rushworth SA, Bowles KM, MacEwan DJ. Bortezomib induces heme oxygenase-1 expression in multiple myeloma. *Cell Cycle*. 2012;11(12):2248-2252.
132. Pham-Huy LA, He H, Pham-Huy C. Free radicals, antioxidants in disease and health. *Int J Biomed Sci*. 2008;4(2):89-96.

133. Birben E, Sahiner UM, Sackesen C, Erzurum S, Kalayci O. Oxidative stress and antioxidant defense. *World Allergy Organ J.* 2012;5(1):9-19.
134. Tripathi AK, Ray AK, Mishra SK, Bishen SM, Mishra H, Khurana A. Molecular and Therapeutic Insights of Alpha-Lipoic Acid as a Potential Molecule for Disease Prevention. *Rev Bras Farmacogn.* 2023;33(2):272-287.
135. Ulrich K, Jakob U. The role of thiols in antioxidant systems. *Free Radic Biol Med.* 2019;140:14-27.
136. Obeng EA, Carlson LM, Gutman DM, Harrington WJ, Jr., Lee KP, Boise LH. Proteasome inhibitors induce a terminal unfolded protein response in multiple myeloma cells. *Blood.* 2006;107(12):4907-4916.
137. Hetz C. The unfolded protein response: controlling cell fate decisions under ER stress and beyond. *Nat Rev Mol Cell Biol.* 2012;13(2):89-102.
138. Lin PH, Chiang MT, Chau LY. Ubiquitin-proteasome system mediates heme oxygenase-1 degradation through endoplasmic reticulum-associated degradation pathway. *Biochim Biophys Acta.* 2008;1783(10):1826-1834.
139. Mamely I, van Vugt MA, Smits VA, Semple JI, Lemmens B, Perrakis A, Medema RH, Freire R. Polo-like kinase-1 controls proteasome-dependent degradation of Claspin during checkpoint recovery. *Curr Biol.* 2006;16(19):1950-1955.
140. Borman S. Fog Clearing On TIC10 Drug Development Mix-Up. *c&en.* 2014;92(23).
141. Greer YE, Lipkowitz S. TIC10/ONC201: a bend in the road to clinical development. *Oncoscience.* 2015;2(2):75-76.
142. Wang S, El-Deiry WS. TRAIL and apoptosis induction by TNF-family death receptors. *Oncogene.* 2003;22(53):8628-8633.
143. Oh YT, Sun SY. Regulation of Cancer Metastasis by TRAIL/Death Receptor Signaling. *Biomolecules.* 2021;11(4).
144. Sträter J, Hinz U, Walczak H, Mechtersheimer G, Koretz K, Herfarth C, Möller P, Lehnert T. Expression of TRAIL and TRAIL receptors in colon carcinoma: TRAIL-R1 is an independent prognostic parameter. *Clin Cancer Res.* 2002;8(12):3734-3740.
145. Pan G, O'Rourke K, Chinnaiyan AM, Gentz R, Ebner R, Ni J, Dixit VM. The receptor for the cytotoxic ligand TRAIL. *Science.* 1997;276(5309):111-113.

146. Liguori NR, Sanchez Sevilla Uruchurtu A, Zhang L, Abbas AE, Lee YS, Zhou L, Azzoli CG, El-Deiry WS. Preclinical studies with ONC201/TIC10 and lurbinectedin as a novel combination therapy in small cell lung cancer (SCLC). *Am J Cancer Res.* 2022;12(2):729-743.
147. Artykov A, Belov DA, Shipunova VO, Trushina DB, Deyev SM, Dolgikh DA, Kirpichnikov MP, Gasparian ME. Chemotherapeutic Agents Sensitize Resistant Cancer Cells to the DR5-Specific Variant DR5-B more Efficiently than to TRAIL by Modulating the Surface Expression of Death and Decoy Receptors. *Cancers (Basel).* 2020;12(5).
148. Liu X, Yue P, Chen S, Hu L, Lonial S, Khuri FR, Sun SY. The proteasome inhibitor PS-341 (bortezomib) up-regulates DR5 expression leading to induction of apoptosis and enhancement of TRAIL-induced apoptosis despite up-regulation of c-FLIP and survivin expression in human NSCLC cells. *Cancer Res.* 2007;67(10):4981-4988.
149. Yan G, Du Q, Wei X, Miozzi J, Kang C, Wang J, Han X, Pan J, Xie H, Chen J, Zhang W. Application of Real-Time Cell Electronic Analysis System in Modern Pharmaceutical Evaluation and Analysis. *Molecules.* 2018;23(12).
150. Lü S, Wang J. The resistance mechanisms of proteasome inhibitor bortezomib. *Biomark Res.* 2013;1(1):13.
151. Politou M, Karadimitris A, Terpos E, Kotsianidis I, Apperley JF, Rahemtulla A. No evidence of mutations of the PSMB5 (beta-5 subunit of proteasome) in a case of myeloma with clinical resistance to Bortezomib. *Leuk Res.* 2006;30(2):240-241.
152. de Wilt LH, Jansen G, Assaraf YG, van Meerloo J, Cloos J, Schimmer AD, Chan ET, Kirk CJ, Peters GJ, Kruijt FA. Proteasome-based mechanisms of intrinsic and acquired bortezomib resistance in non-small cell lung cancer. *Biochem Pharmacol.* 2012;83(2):207-217.
153. Ishizawa J, Kojima K, Chachad D, Ruvolo P, Ruvolo V, Jacamo RO, Borthakur G, Mu H, Zeng Z, Tabe Y, Allen JE, Wang Z, Ma W, Lee HC, Orlowski R, Sarbassov dos D, Lorenzi PL, Huang X, Neelapu SS, McDonnell T, Miranda RN, Wang M, Kantarjian H, Konopleva M, Davis RE, Andreeff M. ATF4 induction through an atypical integrated stress response to ONC201 triggers p53-independent apoptosis in hematological malignancies. *Sci Signal.* 2016;9(415):ra17.
154. Prabhu VV, Talekar MK, Lulla AR, Kline CLB, Zhou L, Hall J, Van den Heuvel APJ, Dicker DT, Babar J, Grupp SA, Garnett MJ, McDermott U, Benes CH, Pu JJ,

Claxton DF, Khan N, Oster W, Allen JE, El-Deiry WS. Single agent and synergistic combinatorial efficacy of first-in-class small molecule imipridone ONC201 in hematological malignancies. *Cell Cycle*. 2018;17(4):468-478.

155. Prabhu VV, Allen JE, Dicker DT, El-Deiry WS. Small-Molecule ONC201/TIC10 Targets Chemotherapy-Resistant Colorectal Cancer Stem-like Cells in an Akt/Foxo3a/TRAIL-Dependent Manner. *Cancer Res*. 2015;75(7):1423-1432.

156. Allen JE, Krigsfeld G, Patel L, Mayes PA, Dicker DT, Wu GS, El-Deiry WS. Identification of TRAIL-inducing compounds highlights small molecule ONC201/TIC10 as a unique anti-cancer agent that activates the TRAIL pathway. *Mol Cancer*. 2015;14:99.

157. Karpel-Massler G, Bâ M, Shu C, Halatsch ME, Westhoff MA, Bruce JN, Canoll P, Siegelin MD. TIC10/ONC201 synergizes with Bcl-2/Bcl-xL inhibition in glioblastoma by suppression of Mcl-1 and its binding partners in vitro and in vivo. *Oncotarget*. 2015;6(34):36456-36471.

158. Bychkov ML, Gasparian ME, Dolgikh DA, Kirpichnikov MP. Combination of TRAIL with bortezomib shifted apoptotic signaling from DR4 to DR5 death receptor by selective internalization and degradation of DR4. *PLoS One*. 2014;9(10):e109756.

9. Bibliography of candidate's publications

9.1 List of publications used for the thesis

1. **Angéla Takács[#]**, Zsófia Szász[#], Márton Kalabay, Péter Bárány, Antal Csámpai, Hargita Hegyesi, Orsolya Láng, Eszter Lajkó, László Kőhidai (2021) The Synergistic Activity of Bortezomib and TIC10 against A2058 Melanoma Cells. Pharmaceuticals (Basel). 14(8): 820

[#] shared first authorship

IF 5.215; Q1

2. **Angéla Takács**, Eszter Lajkó, Orsolya Láng, Ildikó Istenes, László Kőhidai (2020) Alpha-lipoic acid alters the antitumor effect of bortezomib in melanoma cells in vitro. Sci Rep. 10(1):14287

IF 4.380; D1

9.2 List of publications not used for the thesis

1. Matyas Csaba, Trojnar Eszter, Zhao Suxian, Arif Muhammad, Mukhopadhyay Partha, Kovacs, Attila, Fabian Alexandra, Tokodi Marton, Bagyura Zsolt, Merkely Bela, Kohidai Laszlo, Lajko Eszter, **Takacs Angela**, He Yong, Gao Bin, Paloczi Janos, Lohoff Falk W, Haskó György, Ding Wen-Xing, Pacher Pal (2023) PCSK9, A Promising Novel Target for Age-Related Cardiovascular Dysfunction JACC: Basic Trans Science 8(10) 1334

IF: 9,7; Q1

2. Zsolt Bagyura[#], **Angéla Takács[#]**, Loretta Kiss, Edit Dósa, Réka Vadas, Tin Dat Nguyen, Elek Dinya, Pál Soós, Zsolt Szelid, Orsolya Láng, Éva Pállinger, László Kőhidai, Béla Merkely (2022) Level of advanced oxidation protein products is associated with subclinical atherosclerosis. BMC Cardiovasc Disord. 22(1):5

[#] shared first authorship

IF 2.1; Q2

3. Zsófia Kőhidai, **Angéla Takács**, Eszter Lajkó, Zoltán Géczi, Éva Pállinger, Orsolya Láng, László Kőhidai (2022) The effects of mouthwashes in human gingiva epithelial progenitor (HGEPP) cells. Clin Oral Investig. 26(6):4559-4574

IF 3.4; Q1

4. Márton Kalabay, Zsófia Szász, Orsolya Láng, Éva Pállinger, Cintia Duró, Tamás Jernei, Antal Csámpai, **Angéla Takács**, László Kőhidai (2022) Investigation of the Antitumor Effects of Tamoxifen and Its Ferrocene-Linked Derivatives on Pancreatic and Breast Cancer Cell Lines. *Pharmaceuticals (Basel)*. 15(3):314
IF 4.6; Q1
5. Krisztina S. Nagy, Krisztina Toth, Eva Pallinger, **Angela Takacs**, Laszlo Kohidai, Angela Jedlovszky-Hajdu, Domokos Mathe, Noemi Kovacs, Daniel S. Veres, Krisztian Szigeti, Kristof Molnar, Eniko Krisch, Judit E. Puskas (2021) Folate-Targeted Monodisperse PEG-Based Conjugates Made by Chemo-Enzymatic Methods for Cancer Diagnosis and Treatment. *Int J Mol Sci*. 22(19):10347
IF 6.208; Q1
6. Constantinos Voniatis, Lukas Balsevicius, Dóra Barczikai, David Juriga, **Angéla Takács**, László Kőhidai, Krisztina Nagy, Angela Jedlovszky-Hajdu (2020) Co-electrospun polysuccinimide/poly(vinyl alcohol) composite meshes for tissue engineering. *J Mol Liq*. 306:112895
IF 6.165; Q1
7. Kinga Judit Fodor, Dániel Hutai, Tamás Jernei, **Angéla Takács**, Zsófia Szász, Máté Sulyok, Veronika Harmath, Rita Szabó Oláh, Gitta Schlosser, Ferenc Hudecz, László Kőhidai, Antal Csámpai (2020) Novel polycondensed partly saturated b-carbolines including ferrocene analogues: synthesis; DFT-supported structural analysis and mechanism of diastereoselective transformations; a preliminary study on in vitro antiproliferative effect. *Molecules* 25(7):1599
IF 4.412; Q1
8. Hargita Hegyesi, Nikolett Sándor, Géza Sáfrány, Virág Lovas, Árpád Kovács, **Angéla Takács**, László Kőhidai, Lilla Turiák, Ágnes Kittel, Krisztina Pálóczi, Lóránd Bertók, Edit Irén Buzás (2019) Radio-detoxified LPS alters bone marrow-derived extracellular vesicles and endothelial progenitor cells. *Stem Cell Res Ther*. 10(1):313.
IF 5.116; D1
9. Jernei T, Duró C, Dembo A, Lajkó E, **Takács A**, Kőhidai L, Schlosser G, Csámpai A. (2019) Synthesis, Structure and In Vitro Cytotoxic Activity of Novel

Cinchona-Chalcone Hybrids with 1,4-Disubstituted- and 1,5-Disubstituted 1,2,3-Triazole Linkers. *Molecules* 24(22): 4077

IF 3.267; Q1

10. Péter Bárány, Rita Szabó Oláh, Imre Kovács, Tamás Czuczi, Csenge Lilla Szabó, **Angéla Takács**, Eszter Lajkó, Orsolya Láng, László Kohidai, Gitta Schlosser, Szilvia Bosze, Gábor Mezo, Ferenc Hudecz, Antal Csámpai (2018) Ferrocene-Containing Impiridone (ONC201) Hybrids: Synthesis, DFT Modelling, In Vitro Evaluation, and Structure–Activity Relationships. *Molecules* 23(9):2248

IF 3.060; Q1

the cumulative impact factor: 57.623

10. Acknowledgements

First of all, I would like to acknowledge and give my greatest thanks to my supervisors Prof. Dr. László Kőhidai and Dr. Eszter Lajkó, who were my mentors from the beginning and made this work possible. Their guidance and advice carried me through all the stages of writing my thesis.

I would also like to give special thanks to Dr. Orsolya Láng, Dr. Éva Pállinger, Dr. Zsófia Szász, Dr. Márton Kalabay, and last, but certainly not least to Nóra Fekete, Andrea Kovács and Diána Mező for their continuous help and to whom I could always turn to for advice.

A debt of attitude is also owed to Prof. Dr. Edit Buzás for allowing me to work in the Department of Genetics, Cell- and Immunobiology.

Special thanks to all of my colleagues, especially to Dr. Hargita Hegyesi, Dr. Tamás Visnovitz, Anna Koncz, Gyöngyvér Orsolya Sándor and András Försönits who always helped me when I got lost in biology.

I would like to thank Dr. Ádám Zolcsák and Dr. András Szilvay for supporting each other's work from the very beginning.

I am also very grateful to my whole family, to my husband for his endless help, to our son for sleeping well in the afternoons, and to my parents for their continuous support and understanding when undertaking my research and writing my project. Your prayer for me was what sustained me this far.